In vitro bioactivity profile analysis and evaluation of usability of bioactive glass fibers as a structural part in load-bearing implants

Master's Thesis

University of Turku

MSc Degree Programme in Biomedical Sciences

Drug Discovery and Development

December 2020

Niki Jalava

Supervisors: Niko Moritz, Dos

Julia Kulkova, DDS, PhD

Formal Examiner: Ulla-Mari Pesonen, Prof

Institute of Biomedicine

The originality of this thesis has been verified in accordance with the University of Turku quality assurance system using the Turnitin Originality Check service

UNIVERSITY OF TURKU
Institute of Biomedicine, Faculty of Medicine

JALAVA, NIKI: In vitro bioactivity profile analysis and evaluation of usability of bioactive glass fibers as a structural part in load-bearing implants
Master´s Thesis, 46p
MSc Degree Programme in Biomedical Sciences/Drug Discovery and Development
November 2020

Abstract

Metallic and permanent bone implants expose trauma patients to recurring fractures and infections even after years of implantation. Metallic implants also predispose for stress shielding phenomenon and fibrous capsule formation driving the research to find more biocompatible solutions for implant materials and construction. Bioactive materials such as bioactive glasses have proven to be effective at repairing large bone defects, cure and prevent bone infections during the healing process, and they are completely biodegradable.

Our goal is to create novel biodegradable composite implants which are comprised of polymer matrices reinforced with bioactive glass fibres. With such composite, it could be possible to create a load bearing and biodegradable implant that would also be osteoinductive and antimicrobial with customizable degradation time.

For this, we have chosen 3 different types of bioactive glass compositions 1-06, 13-93, and 18-06 that represent fast, medium, and slow bioactivity profiles, respectively, according to the literature. We prepared the glasses, pulled them into fibers and performed a dissolution test and SEM analysis to assess the bioactivity profile of the glasses in fiber form. The secondary goal was to evaluate the usability of these fibers as structural components.

The results from the dissolution test in simulated body fluid and SEM analysis confirmed that the 1-06 glass fibers were bioactive. The 13-93 and 18-06 fibers did not respond to SBF, start leeching ions or form a calcium phosphate layer. However, the 13-93 blocks, that were used as the positive control, did have a stronger response to the SBF than the 1-06. This suggests that the 1-06 fibers might represent a medium bioactivity profile instead of fast. These results might also mean that the 13-93 and 18-06 fibers were not immersed long enough for them to dissolute and they might still represent the suggested bioactivity profiles. Although, the glass composition of the fibers was altered during the fiber pulling process and the fibers had different composition than intended.

Keywords: Bioactive glass, fibers, biodegradable implant

Table of Contents

1. Introduction 1
   1.1 The Introduction and the Structure of Bioactive Glasses 1
   1.2 The Mechanism of Action and the Cellular Responses 3
   1.3 The Antibacterial Properties 6
   1.4 The Processability of Bioactive Glasses 7
   1.5 The Bioactive Glass Fibers, FRCs and Embroidery Technique 9
   1.6 The Bioactivity Profile of Bioactive Glasses 11
2. Materials and Methods 12
   2.1 Materials and the Experimental Design 12
   2.2 Melting of the Bioactive Glasses 12
   2.3 Pulling of the Glass Fibers 13
   2.4 Dissolution Test 13
      2.4.1 Preparation of the Samples 13
      2.4.2 Ion Release 14
   2.5 Scanning Electron Microscopy (SEM) 15
   2.6 Energy-Dispersive X-ray Spectroscopy 16
3. Results 17
   3.1 Ion Release Analysis 17
   3.2 SEM Analysis 19
   3.3 Energy-Dispersive X-ray Spectroscopy 20
4. Discussion 23
   4.1 Assessment of the Bioactivity Profile and Evaluation of the Results 23
   4.2 Fiber Pulling Methodology 24
   4.3 Estimation of Cell Toxicity 26
   4.4 Fiber Reinforced Composites 27
   4.5 Biodegradable FRCs 28
   4.6 Designing Biodegradable Implants 30
5. Conclusions 34
6. Acknowledgements 35
6. List of abbreviations 36
7. References 37

1. Introduction

1.1 The Introduction and the Structure of Bioactive Glasses

The issue of foreign body reactions and rejection to the first-generation biomaterials, such as metallic or plastic materials, in the late 1960s was presented to Larry Hench[1] and he became fascinated by the idea of creating a more biocompatible biomaterial. He hypothesised that if the material could form hydrated calcium phosphate, also known as hydroxyapatite, it might be more biocompatible and not be rejected by the human body[1]. This hypothesis lead to the discovery and development of the second-generation biomaterials, namely bioactive glasses (BG), and ultimately to the invention of 45S5 Bioglass® in the early 1970s[2].

The classic BGs, such as the Bioglass®, are based on the traditional soda-lime-glass composition. They compose of the oxides of silicate (SiO_2), sodium (Na_2O), calcium (CaO), and phosphate (P_2O_5). The main structure of the BGs consists of Si-O backbone where silicon cations are connected by oxygen anions. Each silicon forms a tetrahedra with 4 oxygen atoms and each oxygen is linked to two silicon atoms connecting the tetrahedra together creating an organized interconnected network[3,4]. These oxygens connecting the silicon atoms are called the bridging oxygens (BOs). This kind of structure network is naturally occurring for example in quartz stone which is really hard and chemically stable mineral with low bioavailability of silicon[5]. For this reason, modifier oxygens (MOs), such as Na_2O and CaO, are added to the matrix to break up the dense and highly interconnected structure. These MOs from Si-O-Na^+ and Si-O-Ca^{2+} bonds and create non-bridging oxygens (NBOs) which break the interconnective chain creating more disorder and loosen the structure[3,4].

The main factor that separates vitreous silica from rock-like minerals is the amorphous structure which is created by the loose interconnectivity of the silicate structure. This kind of disruption is essential for any kind of reactivity for a glass, but to achieve bioactivity, the ratio of BO to NBO and the structural components must also be balanced. For example in Bioglass®, Hench used 45 m-% SiO_2, 24.5 m-% CaO, 24.5 m-% Na_2O, and 6 m-% P_2O_5, hence the name 45S5 – 45% Si and 5:1 molar ratio of calcium to phosphate. To achieve reactivity, it is important that liquids such as water can penetrate the glass surface and get into the structure. As the glass starts to dissolve, the ionic composition needs to be suitable for the calcium phosphate formation so that the biological reactions can take place. The general rule is that by decreasing the interconnectivity of the silicate network the reactivity of the BG increases and by increasing the interconnectivity the less reactive it becomes[1,6,7]. This can be described by the Q^n-state of the silicate atoms where the n (n=0–4) equals the number of bridging oxygens connected to the silicon tetrahedra. Most bioactive glasses are largely dominant in the Q^2 species and secondary in Q^3 species due to the MOs disrupting the interconnectivity[3,4,8]. The overall interconnectivity can be

presented by calculating the average number for the Q^n species which translates to the network connectivity (NC) value. According to Mathew *et al.*, NC of 2.1 to 2.6 is the range for optimal bioactivity for BGs[8], and while moving closer to 3 the bioactivity gradually decreases reaching the upper limit of bioactivity at around 2.9[8,9]. However, the loss of bioactivity is more accountable to the increase of Q^4 species rather than the Q^3s. Mathew *et al.*, estimated that over 10% Q^4 species would result in the loss of bioactivity. Usually the characteristics of the glass are modified by changing the ratios of the silicon and the MOs or by changing the surface area of the glass[1,4,10,11]. Addition of sodium or calcium, removal of silicon, increased porosity or smaller particle size increase the reactivity, while the opposite actions or the addition of multivalent cations, such as aluminium, manganese, or titanium, decrease the reactivity[1,4,7,11,12].

Phosphate, however, appears in the glass mostly as orthophosphate lacking any covalent bond to the silicon backbone[3,4,8]. The lack of covalent bonds makes orthophosphate readily available and easily dissolvable from the glass matrix. Orthophosphate content directly increases the bioactivity of the glass when the electronegative charges are balanced with Na^+ and Ca^{2+} ions[8,13]. When the balance is not met, the phosphate starts to form BO bonds to the silicon which actually increases the NC and decreases the bioactivity of the glass, since the covalent bonds need to be hydrolysed before the phosphate can be released[8,13]. The phosphate molecules rarely form more than one BO bond but this is enough to tightly bound them to the structure causing them to no longer contribute to the overall bioactivity the same way as orthophosphate[8,13].

Since the early days, more complex bioactive glasses have been made and now bioactive glass has become an umbrella term for a variety of biocompatible glasses that can bond to bone and soft tissue[2]. The third-generation biomaterials utilize more precisely engineered bioactive materials that aim to cause a specific cellular response at a genetic level, and combines them with medical grade polymers creating composites that better mimic the biological environment of the human body[1,14]. Some third-generation biomaterials use bioresorbable polymers which could provide a fully biodegradable biomaterial, but so far, they have been limited to non-load-bearing applications. The next step for the fourth-generation biomaterials have been speculated to include manipulation of the electrical systems of the cells with the aim of creating even more accurately engineered biological solutions that would improve the integration, better mimic the natural environment of the body, and lower the failure rates of the bioactive implants[14].

Currently, The US Food and Drug Administration (FDA) has approved Bioglass® 45S5 and Bonalive® S53P4 BGs for clinical use as a bone substitute material. Most of the clinical applications utilize the BGs as particulate, usually as such, mixed with a viscous substrate to create a putty, or embedded in a non-resorbable composite matrix when load bearing capabilities are required. These applications can be used to fill in cavities in bones after for example a bone tumour removal or for acceleration of bone

regeneration after traumatic events. These applications show good treatment response in both non-load bearing and load bearing conditions[15–18]. However, the non-resorbable composite materials still may need to be surgically removed after their purpose has been fulfilled requiring more hospital visits and risking a post-surgery infection. This leaves an unmet medical need for load bearing bioresorbable materials that are naturally removed from the body over time.

1.2 The Mechanism of Action and the Cellular Responses

The bone forming effects of bioactive glasses can be separated into two main events – the formation of a calcium-phosphate layer and the promotion of the beneficial cellular reactions[1,12]. When in contact with aqueous solutions like the human extracellular fluid, the water molecules penetrate to the glass, interact with the Na^+ and Ca^{2+} ions, and detach them from the matrix. This means that the BG starts to dissolve as soon as it comes to contact with the aqueous solutions. The water molecules donate their hydroxide group and release NaOH and $Ca(OH)_2$ from the matrix in exchange for the H^+ ions. NaOH and $Ca(OH)_2$ readily ionize in the water releasing the OH^- and raising the local pH. This rapid exchange of ions and increase in pH creates an alkaline environment in which also the basic structure of the glass starts to break. The OH^- ions start to hydrolyse the Si–O–Si bonds and cause the release of silicon from the network[12]. The silicon cations react with the hydroxide anions and start forming silicic acids ($Si(OH)_x^{-4-x}$) which create a layer of silica gel on the surface of the glass. The released silicon then condenses and repolymerises on the surface of the glass forming a scaffold where the released but also endogenous calcium and phosphate can start to precipitate. The $CaO\text{-}P_2O_5$ layer eventually absorbs carbonates and hydroxyls from the extracellular fluid and crystallise into hydroxyapatite (HA)[1,12]. This is a key event for the bone regeneration since HA is the most common mineral in bone and can act as a foundation for the bone cells to attach. Osteoblasts and osteogenic precursor cells can attach themselves to the crystallized calcium phosphate/HA layer and start their natural actions for bone regeneration.

The other key event for bone regeneration is the promotion of osteogenic differentiation and proliferation through activation of cellular mechanisms[19]. The cellular reactions are initiated by the dissolution products of BGs, mainly by the increase in local Ca and Si ion concentrations[20–24].

Ca^{2+} ions are the most important for osteoblast differentiation, proliferation, and bone mineralization[24–28]. Maeno *et al*. tested the cellular response of primary mouse osteoblast monolayer and 3D cultures to differing Ca^{2+} ion concentrations, and the results showed increased proliferation at 2-6 mM Ca^{2+} concentration and increased matrix mineralization and differentiation at slightly higher concentrations of 6-10 mM[24]. Whereas Narita *et al.*, cultured murine osteoblasts in the presence of $CA(OH)_2$ and discovered that the calcium ions caused prolonged activation of p38 and JNK which have an important role in bone mineralization[27]. Calcium acts on the surface of the bone precursor cells through a calcium-

sensing receptor(CaSR) which activates from high extracellular calcium concentration[28,29]. Dvorak *et al.* demonstrated CaSR-related cellular responses in multiple osteoblast cell lines in the presence of extracellular calcium[28]. In their study, the CaSR excitation resulted in the activation of mitogen activated ERK 1/2 pathway and Akt, and the inhibition of GSK3β which affect osteoblast proliferation, the activation of a transcription factor Cbfa1 and its downstream proteins osteocalcin and osteopontin which are key effectors in osteoblast differentiation and mineralization, and the activation of alkaline phosphatase which has a role in bone mineralization.

Silicon is considered an essential micronutrient for bone development and healthy bone metabolism with an effect on osteoblast proliferation and metabolic activity[5,30]. In the study by Rettiff *et al.,* orthosilicic acid ($Si(OH)_4$) promotes collagen type-1 production in human osteoblasts, and has an impact on osteoblastic differentiation shown by the increased alkaline phosphatase and osteocalcin activity[31]. However, they discussed that whether silicon is the direct contributor to the commitment of osteoblastic differentiation and ECM mineralization remains unclear, but regardless silicon undoubtedly has a positive effect for bone formation and metabolic activity of osteoblasts. Furthermore, silicon has inhibitory effects on bone resorption through induced secretion of osteoprotegerin and subsequent inhibition of RANKL activity which leads to reduced osteoclasts maturation and activation[32,33], indirectly enhancing the regenerative processes.

Additionally, while having a bigger impact for the bone regeneration through calcium phosphate crystallization, inorganic phosphate has an effect through ERK1/2 pathway which activates the transcription factor Fra-1[34]. Julien *et al.* suggested that Fra-1 has a role in the activation of matrix Gla protein (MGP) which is an important regulator in bone mineralization[34]. In their study, they discussed that MGP overexpressing mice show improper bone mineralization, and that Fra-1 overexpressed mice develop osteosclerosis while Fra-1 deficient mice develop osteopenia[34]. Through this pathway, phosphate released from the BG can regulate the cell metabolism of osteoblasts and promote proper mineralization of the bone.

These dissolution products also upregulate multiple other factors either directly or indirectly. These include transcription factors, cell-cycle regulators, signal transduction pathways, growth factors, DNA repair proteins, apoptosis regulators, ECM related proteins, and differentiation markers[1,20–23,26]. Xynos *et al.* identified over 100 upregulated mRNA species in human osteoblasts when cultured with in the presence of 45S5 BG, and of those mRNA species, 60 were recognized to have increased 2 to 7-fold in contrast to the control[22]. The upregulation of mRNA species indicate activation of genes, and in this case, they were found to be specifically beneficial for osteoblast differentiation, proliferation, and viability. Furthermore, the genes synergise well with each other enhancing and complementing simultaneous and consecutive signalling pathways and cellular processes.

According to Xynos *et al*.[22], some of the upregulated transcription factors are osteoblast specific, such as RCL growth related c-myc, c-jun and fra-1. These transcription factors are responsible for transitioning the osteoblast precursor cells from the stationary G0 phase into the active G1 phase which prepares the cell for replication. Furthermore, three different cell cycle regulators which allow the progenitor cells to pass specific cell cycle checkpoints and lead to DNA replication and eventually mitosis were also upregulated[1,21,23]. Cyclin D1, which is responsible for the crucial transition from G1 phase to DNA synthesis phase (S phase), was up regulated by 400%. Two other cyclins, cyclin K and CDKN1A, which are responsible for early stages of mitosis were upregulated by 200 and 350%, respectively.

The DNA synthesis and replication processes during the S phase are fragile and prone to error due to the sheer amount of actions happening during the duplication and recombination. Therefore, different DNA repair proteins are present during the replication phase to facilitate error correction during the recombination and complete DNA replication. Xynos *et al*. identified multiple upregulated DNA synthesis, repair, and recombination protein coding genes in their study[22]. DNA exclusion repair protein, mutL protein homolog, and HMG-1 are examples of the upregulated proteins that are ensuring complete DNA synthesis.

While it is important that the cell pass the required cell cycle phases and differentiate into osteoblasts, it is equally important to clean out the cells that are incapable of dividing and only leave the cells that lead to bone growth. Upkeeping of the incapable cells is draining energy and nutrients from the differentiated cells, and therefore it is highly beneficial to eliminate the incapable cell by apoptosis to recycle nutrients and proteins from these cells. The upregulated genes by the BG dissolution products include multiple apoptosis regulators, such as DAD1, calpain, and deoxyribonuclease II, which are responsible for elimination of the incapable cells[21,23].

Additionally, different growth factors and signal transduction pathway inducers can promote the osteogenic progenitor cells to differentiate and osteoblasts to grow and proliferate. Some of these potent growth factors such as insulin-like growth factor II (IGFII), vascular endothelial growth factor (VEGF), macrophage colony stimulating factor (MCSF), and bone-derived growth factor are upregulated by BG[21,22,26]. Signal transduction pathway inducers, such as MAPKAP kinase 2, are also upregulated further more proving the synergistic effect of the BG dissolution products have on bone regeneration[22].

Another good marker for matured and viable osteoblasts is that the cells start to produce collagen and other ECM compounds. The upregulated cell differentiation markers and ECM related protein genes are proving that the cells undergo changes which lead to bone formation. Osteoblasts cannot produce actual bone nodules, so they need to specialise and differentiate into osteocytes. According to Xynos *et al.,* the most upregulated gene is the cell surface antigen CD44 which is an osteocyte specific marker[22]. The 7-fold increase in CD44 expression implies that the osteoblasts are further differentiating into mature

osteocytes that are capable of forming bone nodules. In addition, the ECM production related genes such as matrix-metalloproteinase 2 and 14, TIMP2, and bone proteoglycan 2 precursor are upregulated which proves that the cells are active and producing matrix related components[21–23]. In conclusion, the BG does not only provide a biological scaffold for bone regeneration but also actively promotes cell maturation and bone formation through cell signalling and gene activation. While it is not clear if the BG dissolution products are specifically activating all of these genes or are some of them results of normal cellular downstream signalling cascades which have been activated by BG, it is certain that BGs guide bone cells towards proliferation and regeneration.

1.3 The Antibacterial Properties

The most prevalent challenge associated with the treatment of bone cavities is the management of infections. Since bone defects or cavities often lack sufficient blood supply because of damaged blood vessels, the defects are often immunocompromised and filled with coagulated blood and extracellular fluid which offer ideal conditions for bacteria to thrive and spread. This makes BGs a very feasible treatment option in the clinical setting since it is also antimicrobial[18,35–39]. Munukka *et al.* tested the antimicrobiality of several BGs on 29 clinically important aerobic bacteria and all the BGs had bactericidal or bacteriostatic effects on all or most of the bacteria[35] with some variation depending on the glass composition, bacterial species, and time of exposure. However, the bactericidal effect was proven on both gram-negative and gram-positive species. One of the glasses they had used, 13-93, is also being used in the present study as the positive control glass. In the tested *in vitro* environment, it demonstrated bactericidal effects on all but the most resistant strains and at least bacteriostatic of growth inhibiting effect on all of the bacterial strains.

The antimicrobiality of BGs is fully physiological and it is caused by the drastic changes in the local microenvironment. The dissolution products from the BG locally increase the pH and osmotic pressure and make the area around the glass unsustainable for the bacteria and other microbes. The high osmotic pressure drives water out of the bacterial cell causing them to shrink and dry due to the reverse osmosis. The shrinkage can cause development of holes to their cell membrane which leads the to the collapse and death of the cell[36]. The high pH causes distractions to the membrane potential and therefore cellular activity and metabolism decreasing their viability.

The environmental changes are caused by the dissolution of the mineral oxides and ionization of water molecules. By the mechanism explained in the part 1.2, the water molecules act as a nucleophile and break the bonds between the alkanes and the oxygen that connects them to silicon by donating the proton to the connecting oxygen and releasing NaOH or $Ca(OH)_2$. These hydroxides readily ionize in aqueous environment releasing the hydroxide which directly increases the surrounding pH.

Simultaneously, the released sodium, calcium, and phosphate locally increase the osmotic pressure in the area since these ions are also naturally present in the ECF.

Bioactive glasses are also able to target bacteria which have developed a protective biofilm[37,40]. Biofilms are often formed on abiotic prostheses and the surrounding tissues around it by infectious bacteria that have adhered on a surface. These bacteria start secreting extracellular polymeric slime and extracellular DNA which aggregate and form a protective polysaccharide layer, all while the initial bacteria grow and start forming a highly organized multi-layered bacterial colony of several different species which can send clusters to infect other sites[41]. Biofilms cause issues for infection treatment because the antibiotics and immune cells cannot affect the bacteria from under the protective layer of polysaccarides[41,42]. Bioactive glasses can damage the biofilm and therefore expose the bacteria[36,37,40]. This can also be useful for example in combination therapy which involves antibiotics and the bioactive glass. In combination therapy, antibiotics can target the healthy tissue around the bone defect while the bioactive glass has its effect inside the defect. This is further improved by the BG's ability to induce angiogenesis via upregulation of VEGF in fibroblasts[21,43], since the better vascularity will provide better inflow of antibiotics and immune cells to the defect area.

1.4 The Processability of Bioactive Glasses

The BG's ability to bond to bone and create incredibly synergistic cellular responses is what makes BG so efficient in repairing large bone defects like cavities[18,44] and allows substantial bone reformation operations[15]. However, the usability of BGs in the clinical setting is currently largely limited by the poor processability of the glasses[1,11,12,45–47]. The commercially available BG products mostly utilise BGs as particulate which limits their usage to non-load bearing applications such as fillers for bone cavities. Clinically usable BG applications should fulfil certain qualities to be suitable for various situations. Clinical biomaterials for bone healing should present a high number of interconnected pores to allow bone cells and fluids to flow freely throughout the material, but also have structural properties mimicking that of damaged area so it can serve as a proper supporting scaffold for the natural healing of the bone[1,12,48,49]. The dissolution rate should also be aligned with the speed of the tissue regeneration so that the material keeps its shape until the new tissues can take the load. These are the fundamental qualities that a BG application should have, but for it to be also commercially feasible, ease of manufacturing and replicability should also be considered.

The issue with the traditional soda-lime glasses, such as 45S5 and S53P5, is that they crystallize easily at high temperatures which limits their usability to monoliths and particulate[1,4,11,46,47,50]. Because of the amorphous and loose structure of the glasses, they have a tendency to crystallise at certain temperature which is called the crystallisation temperature (T_c)[8,50–52]. At the T_c, the glass structure finds the lowest

state of the energy expenditure which causes densification of the structure increasing the NC and cross-linkage of silicon atoms, and in the case of BGs, this also leads to decreased bioactivity[8,9,11]. The glass transition temperature (T_g), in which the vitrification happens, is usually 100-400 °C below the T_c. However, the glasses are usually heated up to the liquidus temperature (T_l), in which the glass is completely liquified, because at the T_l and more, a more homogenous glass composition is acquired due to better diffusion of the ingredients. In melt-cast glasses, the crystallization is often avoided by rapid cooling or heating of the glass well past the T_c so there is not enough time for crystallization to occur.

However, more advanced techniques have to be utilized to achieve more complicated and porous forms of the BG. The difference between the T_g and the T_c is often referred as the working range ($\Delta T = T_g - T_c$), and the wider this is the easier glass processing techniques can be applied without the glass crystallizing. For example, sintering and fiber pulling require certain viscosity parameters to be effective, and if the glass starts to form small crystals or harden at various locations, the processing becomes hard or impossible. Consequently, a wide working range is a necessity.

The crystallization tendency is directly related to the NC of the glass. Meaning that glasses with more open structure with less interconnectivity will crystallise earlier when heated than glasses with more cross-linked and dense structure[8,9,46,50]. Therefore, the working range can be altered by changing the structural network either by affecting the network connectivity or by changing the MO composition[1,53–56]. By increasing the NC, the looseness in the structure and the molecular tensions in the structure are decreased which makes it less prone to crystallisation. Addition of silicon has been proven to widen the working range of the glasses[4,8,54]. The other ways that have been found to increase the working range and viscosity were to increase the alkaline earth/alkali metal ratio by removal of alkali metals and increase in alkaline earth metals. High alkali content glasses have been recognised to have higher viscosity compared to glasses with higher alkaline earth to alkali metal ratio which raises the T_g and decreases processability[54].

Brink and others demonstrated that by utilizing the mixed alkali effect the working range can be further expanded[54–56]. By substituting Na_2O with K_2O or Li_2O, the different ionic radii and ionic weight of the substitutions change the structural density of the matrix while retaining the change balance and network connectivity[54,55]. According to Tylkowski and Brauer[55], the mixed alkali effect causes a decrease in the structural density, thus affecting the processability. Lithium has smaller ionic weight than sodium, but regardless of its also smaller ionic radius, it causes a net decrease in the density. Similarly but oppositely, potassium has a higher ionic weight than sodium, but its bigger ionic radius expands the structure and causes a net decrease in the density. Even though lithium and potassium have vastly different sizes and weights, they both have a similar effect on the thermal and physical properties of the glass causing a decrease in the T_g and increase in the T_c significantly improving the processability[54–56].

Similar substitutions to the alkaline earth metal oxides causes comparable effects. Substituting CaO with MgO, the structural density decreases because of larger ionic radii of magnesium, and therefore improves the processability of the result glass[57]. However, magnesium can to a degree incorporate to the silicon structure and from BO bonds as a tetrahedra and consequently increase the NC at those sites[57]. According to the Watts *et al.*, approximately 14% of the added magnesium usually acts as a network former regardless of the added amount[57]. Similar reaction can also be predicted with zinc as it has almost the same ionic radius as magnesium. Strontium substitution did not improve the processing window although it decreased the T_g it happened simultaneously with a decrease in the T_c[58,59]. Aluminium and titanium oxides can also be effective at widening the working range if kept at low contents so that the bioactivity remains largely unaffected[51,53,54,60].

Another factor to consider is type of crystals the used glass tends to form. There are multiple types of crystals that can form from the materials in BGs but usually only two of them are relevant – sodium-calcium-silicate (NCS) and calcium-silicate (wollastonite)[10,46,50]. According to Arstila *et al.,* generally the bioactive glasses crystallise to either type of these and it can be considered as an indication of the working range of the glass. Glasses that tend to crystallise into NCS typically have their T_g at around 550 °C and T_c at 600-750 °C, while those glasses that tend to crystallise into wollastonite have their T_g at around 600 °C and T_c at around 850- 930 °C indicating a much larger working range for the latter[10,46,47].

However, it is important to remember that as the amount of silicon and interconnectivity is raising, also the bioactivity and rate of dissolution are decreasing. Therefore, it is always going to be a compromise between optimal bioactivity and processability, and the balance has to be found depending on the intended use or the desirable processing method.

1.5 The Bioactive Glass Fibers, FRCs and Embroidery Technique

Once the suitable working range has been found, bioactive glass can be processed without it losing its bioactivity. The processability allows the glass to be e.g. sintered at high temperatures to achieve porous scaffolds, processed into microspheres, or pulled into fibers[56,60,61]. The glass fibers are an attractive form of bioactive glass since from fibers it is possible to produce porous scaffolds; woven fabrics, strips, or threads; or implants with elastic properties. For example, fibers of bioactive glasses have been effectively used in neuroregeneration[62], for weaving cloths which were wrapped around a defect to improve bone regeneration and wound healing[63], to stimulate full-size skin wound healing[64], and theoretically, they could be used to produce hollow BG fibers that could be used as a drug delivery vector[65].

Glass fibers can be combined together with a polymer matrix to create fiber reinforced composites (FRC). For example, in dentistry FRCs have been in development from 1960s and used in the clinics today[16,66].

By reinforcing the polymer matrix with and glass fibers, it is possible to achieve new materials which are far more durable than the original materials and which can withstand more stress and torque. Additionally, the mechanical properties of the FRCs can be accurately engineered to the be more suitable for the various needs of a medical implant by changing the ratio of polymer to glass fibers or by using different polymer and glass compositions.

The current implant materials used for fixation in bone reconstruction processes are mostly bioinert and biostable. Meaning that they will either stay in the body or require a secondary surgery to be removed after their initial purpose has been fulfilled. Additionally, an issue can arise if the implant material is too stiff. The bone might be exposed to stress shielding, a phenomenon commonly associated with metallic implants such as titanium[16]. During stress shielding, the rigid implant takes the load off of the bone and the body recognizes the bone mass around the implant as unnecessary and starts to recycle it for reuse elsewhere. This causes recurring fractures, implant detachment, inflammation and ultimately surgical removal and a new reconstruction operation.

It is beneficial to search for better alternatives to the metallic implants. The ideal option would be fully degradable implants but currently no such material is in commercial use. However, promising approaches that are in the right direction have been developed. Skull implants produced by Skulle Implants Oy (Turku, Finland) utilize porous composite casing made of inert fiberglass embedded into a polymer matrix and S53P4 bioactive glass laminated between the composite layers[17,66–68]. This solution is osteoinductive, allows bone ingrowth into the material and complete integration while mimicking the physical properties of a natural bone. While this kind of inert casing is required for large defects that would not heal by themselves, the permanent material leaves the area of injury prone to infections and inflammation[67], suggesting that better alternatives could be pursued for smaller scale bone reconstructions. Fiber reinforced composites have been successfully used with bioactive glasses[16,17,60,66]. However, few have been able to successfully combine bioactive glass fibers with a polymer matrix[60]. It would be beneficial, if bioactive glass fibers could be bound into the composite itself because that would open up more possibilities for utilizing bioactive glass.

Another promising application could be the medical embroidery techniques. They have been successfully used in tissue engineering applications using e.g. synthetic polymer threads and collagen fibers[52,69–71]. The embroidery techniques used in scaffold production are most often CNC assisted, automated processes in which the machine is programmed to weave the fibers into the desired shape[69]. Embroidery provides an interesting option for the production of solid but still porous scaffolds if strong enough BG fibers could be created and used as the source material. This would allow for fully computerized and automated prototype modelling that would make mechanical testing and sample production easy while automatically offering a feasible mass production possibility for commercial implants.

1.6 The Bioactivity Profile of Bioactive Glasses

In this study, three different types of bioactive glasses were used – 1-06, 13-93, and 18-06. These glasses have been developed at the Åbo Akademi University in Turku. They represent fast, medium and slow bioactivity profiles, respectively, according to the system created by Vedel *et al*[47]. They developed a computerized method for optimizing bioactive glass properties which can he used to create novel bioactive glasses with desired properties. The three different glasses that were chosen for this study represent wide working range with but differing bioactivity profiles and compositions.

In Vedel's study, the assessment of the bioactivity profile was calculated based on the changes in pH, phosphate concentration, and the thickness of the calcium phosphate layer during a 72h immersion in simulated body fluid (SBF)[47]. The change is pH was used to assess the speed at which the ions were releasing from the glass matrix, the change on phosphate concentration was used to assess the reaction rate, and the development speed of the calcium phosphate layer was used to determine a bioactivity number for the glasses.

The knowledge of the bioactivity profile can be useful for predicting the behaviour and usability of the BGs *in vivo*. Since the glass processing techniques may affect the properties of the glasses, it is necessary to assess the bioactivity profile also for processed glasses.

The purpose of this study is to produce fibers from 1-06, 13-93, and 18-06 bioactive glasses and assess their bioactivity profiles and their usability for load bearing implants. The ultimate goal is to find the most feasible composite material that could be used to create load-bearing implant that would support bone ingrowth and help with bone healing but also dissolve after its purpose has been fulfilled.

2. Materials and Methods

2.1 Materials and the Experimental Design

The BG 1-06 represents the fast bioactivity profile in this study. It has the lowest silicon composition, 50 wt%, of the experimental glasses but also the highest calcium composition of 22 wt%. Therefore, it should the fastest dissolving and the most responsive to aqueous environment due to its low amount of Q_3 -species in the structure, but also the high Ca/Na-ratio increases the bioactivity. 1-06 bioactive glass is expected to form a thick layer of calcium phosphate (CaP) during the study period.

The BG 13-93 is a relatively old type of bioactive glass that was developed in 1993, and it is well known for its bioactivity and large working range[11,47,54,61]. Vedel *et al.* also considered it as a control in their study[47]. According to also Vedel *et al.*'s computerized method, 13-93 BG has medium bioactivity and wide working range. 13-93 has 53 wt% silicon and little lower Ca/Na ratio than 1-06. The 13-93 fibers are expected start showing signs of CaP-layer formation during the study period but still maintain their integrity.

The BG 18-06 BG represents the slowest bioactivity profile and has the highest silicon composition of the experimental glasses at 65 wt%. 18-06 also has a really small Ca/Na ratio indicating a slow response to the aqueous solutions, but according to Vedel's calculations, 18-06 should still be bioactive and resorbable. The 18-06 BG fibers are not expected to have any signs of CaP formation but possibly start to show signs of dissolution during the study period.

For the evaluation of the bioactivity profile, 168 hour immersion in SBF is utilized with the sample collection points at 4, 8, 12, 24, 72, and 168 hours. In contrast to the Vedel's method, pH measurements were omitted and replaced with the direct measurement of the ion concentrations of sodium, silicon, and calcium. The phosphate concentration was measured and used to assess the reactivity rate. The thickness of the CaP-layer was measured with a scanning electron microscope. 13-93 blocks were used as the positive control and the benchmark for the bioactivity profile according to the Vedel *et al.*'s study[47]. Inert E-glass was used as the negative control.

2.2 Melting of the Bioactive Glasses

The bioactive glasses were made in collaboration with Åbo Akademi University. The compositions are summarized in Table 1. The BGs were manufactured using the traditional melting method using a laboratory furnace and a platinum crucible. The same method has been utilized for BG production in multiple studies[10,50,54,72–74] The ingredients were laboratory grade Na_2CO_3, K_2CO_3, MgO, $CaCO_3$, $CaHPO_4$, B_2O and SiO_2 (Thermo Fischer Scientific Oy, Finland, Vantaa). The ingredients were weighed according

to the Table 1 separately for each type of glass, mixed thoroughly, and melted at the furnace at 1360°C for 3 hours. After the 3 hours, the melt glass was casted in a monolith-shaped ceramic mould and set to cool slowly in a secondary oven at 520°C to prevent it from shattering due to rapid shrinking after thermal expansion. The power was cut from the secondary oven after 2 hours and glass plate was collected the next morning.

To achieve homogeneity, each BG plate were shattered after they had set at room temperature and the shards were re-melted and cooled using the same protocol as in the first melting.

Table 1. Compositions of the used bioactive glasses. Ingredients as wt%.

	1-06	13-93	18-06	E-glass
SiO_2	50.0	53.0	65.0	53.0
Na_2O	5.9	6.0	18.4	<1
CaO	22.6	20.0	15.0	11.0
P_2O_5	4.0	4.0	-	-
K_2O	12.0	12.0	-	<1
MgO	5.3	5.0	0.1	11.0
B_2O_3	0.2	-	1.5	10.0
Al_2O_3	-	-	-	14.0

2.3 Pulling of the Glass Fibers

For the fiber pulling, the produced glass monoliths were shattered and re-melted again at the platinum crucible at the 1360 °C. The fibers were pulled manually from the crucible using a ceramic rod. There was no method for monitoring the temperature of the glass melt, so after we removed the glass melt from the furnace, the viscosity of the glass was tested with the ceramic rod and the pulling was started when the melt had congealed enough that the viscosity allowed pulling of the glass without the fiber breaking. Because of the multiple cooling and re-heating cycles, we determined a maximum of four re-heatings per glass melt was allowed before the crystallisation of the glass started to disturb the pulling process and the quality of the glass.

2.4 Dissolution Test

2.4.1 Preparation of the Samples

A novel method was created for preparing the samples for the dissolution test. Fusion deposition modelling (FDM) technique was used to create a scaffold that would fix the fibers in place so that they would be consistent and easier to handle during the tests. The scaffold composed of a series of 4x4 mm

(2,9x2,9 mm inner diameter) rectangles that were connected with a spine that linked the rectangles together (Figure 1). The scaffold was produced from commercial PLA (Clas Ohlson) and the 3D-printer used was a MiniFactory 3D-printer (miniFactory Oy LTD, Seinäjoki, Finland).

First, four layers were printed on the print-surface glass. Since the PLA sticks strongly to the glass, a thin layer of general adhesive (Erikeeper, Oy Sika Finland AB, Espoo, Finland) was used to coat the surface glass substrate to facilitate removal of the printed scaffold without damaging it. After the fourth layer, the printing was paused and a bundle of glass fibers (~15 fibers) was placed on the scaffold. The fibers were fixed to the enlarged wings at both ends of the scaffold with double-sided tape (3M). Afterwards, the print was finished by printing three layers of PLA on top of the fibers which fixed the fibers to the scaffold.

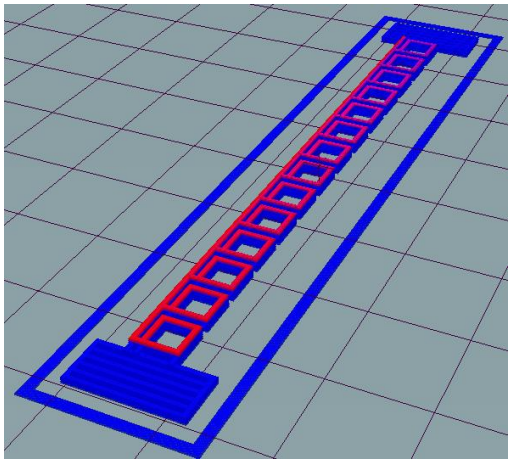

Figure 1. Concept picture of the 3D-printed scaffold.

The fiber bundles were prepared manually by picking and cutting fibers of roughly equal thickness. The fiber bundles were fixed in place with double sided tape (3M) from both ends on a thin clear film. The film was cut out under the fibers leaving the film only to the ends. The thicknesses of the fibers were 0.12 mm for 1-06 and 18-06 and 0.07 mm for 13-93. Thickness of the E-glass fibers used as a negative control was 0.01 mm and the 13-93 used as a positive control were 1.0 mm.

2.4.2 Ion Release

For the ion release test, simulated body fluid (SBF) was prepared according to the Kokubo and Takadama's method[75], and the printed scaffold was cut into singular rectangular glass fiber samples. The correct SBF amount was calculated according to the Equation 1 which was taken from the Kokubo and Takadama's article. The calculated amounts per one square was 16.4 ml for 1-06 and 18-06, 12.3 ml for 13-93, 10,0 ml for E-glass and 1,0 ml for 13-93 blocks. For the 1-06 and 18-06, two squares were used and the used amount of SBF per specimen was 32.8 ml, and for the 13-93, three squares were used

in 36.9 ml SBF. For 13-93 blocks, 10 blocks were used to increase the amount of SBF to 10,0 ml so that it has some buffer to take samples. For the E-glass, one square was used in 10,0 ml SBF. Three replicates were used for the bioactive glass specimens, two replicates for the E-glass and one for 13-93 blocks.

Equation 1. Volume of the SBF needed for the tests. x= number of fibers, r= radius of a fiber, [r]=mm, l=length of the fiber, [l]=mm, R = ratio number.

$$V_s = \frac{A}{R} = \frac{x2\pi rl}{10\frac{mm^2}{ml}}$$

The calculated amounts of SBF were pipetted to factory sterilized 15 ml Falcon tubes (VWR International Oy, Helsinki, Finland) with sterile pipet ends. The other used instruments and the specimens were immersed in 70% EtOH for 5 minutes prior and air dried in fume hood until dry. The specimens were immersed in SBF and the tubes were places in a water bath shaker at 37 °C. A 1.0 ml sample was taken from each tube at 4, 8, 24, 72, and 168-hour time points. The samples were placed into 1.5 ml Eppendorf tubes that were first sterilized in 70% EtOH. The samples were stored in a refrigerator at 5 °C until the analyses began.

The SBF samples were analysed with inductively coupled plasma optical emission spectroscopy (ICP-OES) at Åbo Akademi University. For the ion release analysis, the samples needed to be diluted in 1:9 ratio, so 0.9 ml of the SBF sample was taken and diluted to 8.1 ml of purified water in a clean 15 ml Falcon tubes (VWR International Oy, Helsinki, Finland).

2.5 Scanning Electron Microscopy (SEM)

After the immersion 168-hour immersion in SBF, the specimens were rinsed with purified water, transferred to a well plate, and placed to dry in a heat chamber at 37 °C. The samples were prepared for SEM after 48 hours. From each group, one sample was prepared for cross-sectional images and the remaining two for surface images.

The cross-sectional samples needed to be embedded into resin to achieve a clean cut from which the thickness of the calcium phosphate layer could be measured. For the embedding, a rectangular-shaped mould was created from Lab Putty silicone and hardener (Coltène/Whaledent AG, Altstätten, Switzerland) using a rectangular wooden spacer. After the mould had hardened for 48 hours, immersed specimen was fixed into the mould using a staple to keep it from moving during the pouring of the resin. 20 g of resin and 8 g of hardener (RSF 816, Axson Technologies, Baar, Switzerland) was mixed in a vacuum mixer (THINKY – Planetary Vacuum Mixer: 1000 rpm, 4.5 mb, 5 min) to remove excess air bubbles. After pouring the resin into the moulds, the moulds were placed into vacuum oven (Memmert) for 1 hour (10 mb, 25 °C) and during this time, the pressure was briefly reset to normal every 15 minutes

to reduce the size of bubbles that formed and prevent overflowing. After the first hour, the temperature was increased to 60 °C and the pressure was returned to normal air pressure for 2 hours to hasten the polymerization process. The resin was then left to polymerize for 96 hours in RT.

The fully polymerized resin was cut with a histological saw (2200 rpm, 0,5mm/s) in the middle of an immersed sample so that the cross section of the fibers could be revealed. After cutting, the cross-sectional part was polished with a sanding device with #1000 and #4000 roughness sandpaper while using EtOH as the lubricative liquid until the surface was clean and reflective. All of the samples were then coated with carbon to achieve a conductive surface for the SEM. The coating was done in high-vacuum chamber and with a carbon thread while the specimens were fixed on a small stand.

Representative images of the surface and cross-sectional samples were taken with SEM. The images for the surface images were taken with the smallest magnification (x220-245) and x700 magnification, and for the cross-sectional images, the smallest and x900 magnification was used. The thickness of the calcium phosphate layer was measured manually from the taken images and transformed to the actual scale.

2.6 Energy-Dispersive X-ray Spectroscopy

An Energy-dispersive X-ray Spectroscopy (EDS) was conducted simultaneously with the SEM to determine the elemental compositions of the immersed fibers and to confirm the formation of CaP. Images were taken from five to six fibers from all experimental glass types, and the spectroscopy was performed in the middle and the edge parts of each fiber and additionally on all other visible layers if present. The compositions of the glasses were also calculated from the data.

3. Results

3.1 Ion Release Analysis

Ion release analysis was done with ICP-OES, and the results are shown in Figures 2-5. The analysis was done to silicon, sodium, phosphorus, and calcium ions over 4, 8, 24, 72, and 168 hours.

The baseline for silicon in SBF is 0 mg/l and the changes in SBF silicon concentration are in figure 2. A steady exponential decrease in the release of silicon can be seen from 13-93 blocks. The release curve of 13-93 block has a steep initial slope to 5.1 mg/l in the first 24 hours which then gradually declines to a flatter curve while still slightly increasing at 6.5 mg/l at 168 hours. 1-06 releases silicon at near constant rate to 1.6 mg/l at 72 hours and is still increasing at 2.5 mg/l after 168 hours. 13-93, 18-06 and E-glass do not release silicon ions even after 168 hours of immersion and present a flat curve at 0.0 mg/l until the end of study period.

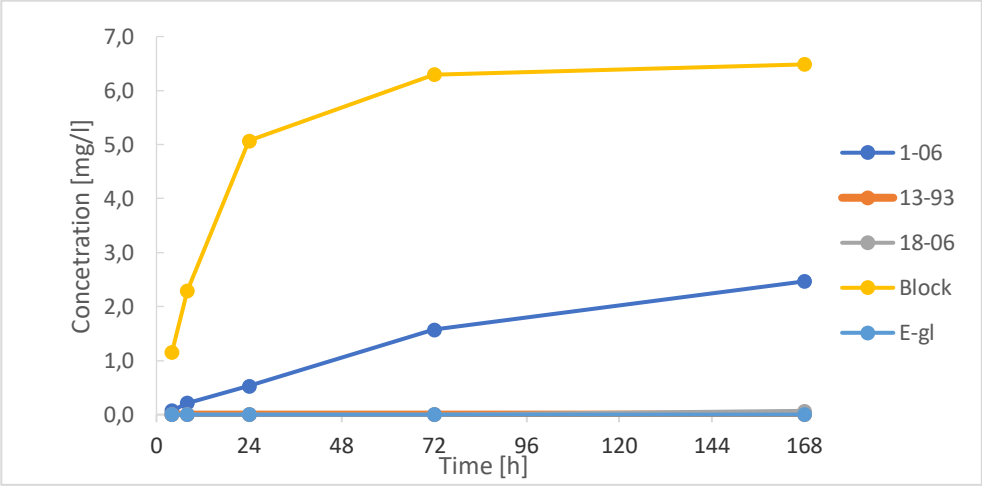

Figure 2. Si-ion concentration of 1-06, 13-93, 18-06, and E-glass fibers and 13-93 bioactive glass blocks in SBF over time.

The measured baseline for the phosphorus concentration in SBF is 3.6 mg/l, and the changes in the SBF phosphorus concentration can be seen in the Figure 3. The changes in the phosphorus concentration are due to the phosphorus being bind into the calcium phosphate layer that is forming on the surface of the bioactive glasses. The 13-93 blocks decrease the phosphorus concentration at a steady rate of 23 µg/l/h and reach 0.0 mg/l in 168 hours. Also, the 1-06 fibers decrease the phosphorus content at a steady rate, approximately 12 µg/l/h, and reach 1.8 mg/l in 168 hours. The 18-06, 13-93 and E-glass fibers maintain the baseline phosphorus concentration throughout the test period.

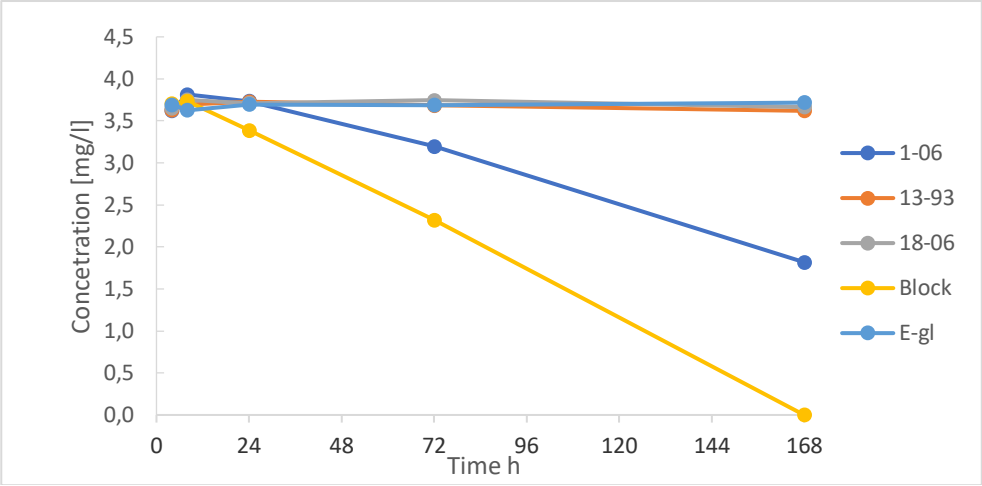

Figure 3. P-ion concentration of 1-06, 13-93, 18-06, and E-glass fibers and 13-93 bioactive glass blocks in SBF over time.

The measured baseline calcium ion concentration in SBF is 10.2 mg/l and the changes of the calcium concentrations are showed in the Figure 4. The SBF and the bioactive glasses contain calcium so both can contribute to the measured calcium concentration. 13-93 blocks present a quick initial release of calcium until 24 h to 15.2 mg/l, followed by a small decrease in concentration at 15.0 mg/l at 72 h, and continuing increasing up to 16.8 mg/l by the 168 h. 1-06 fibers increase the calcium concentration up to 11.0 mg/l for 24 h which then starts to decrease at a near constant rate below the baseline down to 8.8 mg/l by the end of the test period. 13-93, 18-06, and E-glass fibers again present a similar curve to each other; a small initial increase during the first 8 h up to 10.4 mg/l and then staying constant close to the baseline for the rest of the test period.

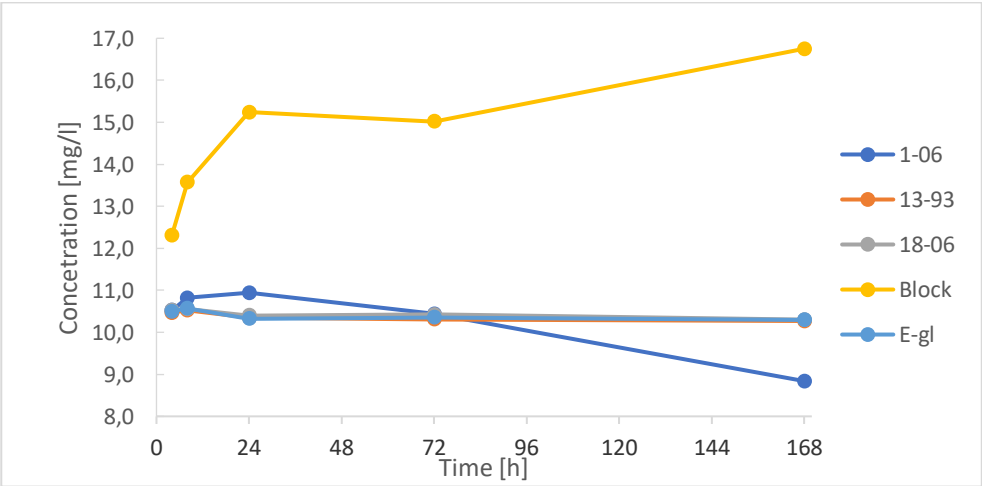

Figure 4. Ca-ion concentration of 1-06, 13-93, 18-06, and E-glass fibers and 13-93 bioactive glass blocks in SBF over time.

The measured baseline for the potassium concentration is 20.8 mg/l, and the changes in the potassium concentration in the SBF can be seen in the Figure 5. The 13-93 blocks had a rapid increase in the potassium concentration to 26.1 mg/l over the first 24 h and gradually smoothening the increase and reaching 32.7 mg/l at 168 h. 1-06 had a faster initial increase reaching 21.6 mg/l over the first 24 h and then at a slightly slower rate increased to 22.6 mg/l over the rest of the test period. 13-93, 18-06, and E-glass fibers had a similar curve though out the study period. They presented an initial increase to 21 mg/l during the first 8 hours until reverting back to baseline level at 24 h for the rest of the test period.

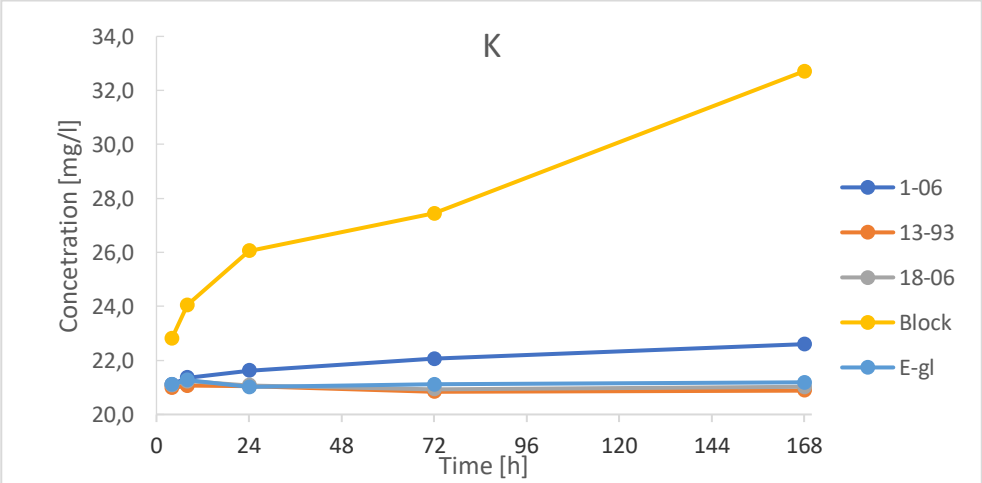

Figure 5. K-ion concentration of 1-06, 13-93, 18-06, and E-glass fibers and 13-93 bioactive glass blocks in SBF over time.

3.2 SEM Analysis

The SEM analysis of the immersed bioactive glass fiber samples reveals the formation of surficial calcium phosphate layer. The surface images are presented in the Figure 6 and the cross-sectional images are in the Figure 7.

In the Figures 6A, 6B, 7A, 7B, a thick layer of calcium phosphate has formed on the surface of the 1-06 fibers. Calcium phosphate covers the whole surface area of the fibers, and the layer is approximately 16.6 µm (SD = 4.6 µm, n = 20) thick. The calcium phosphate layer has cracked in multiple positions, possibly due to shrinking during the drying process. The calcium phosphate layer also has multiple differently sized granules on its surface. From the cross-sectional images (Figures 7A, 7B), definite four-phase layering can be observed – an intact untransformed glass in the middle, a darker silicon-rich section above the middle, a transition layer between the Si-rich area and the calcium-phosphate layer above that, and the calcium-phosphate layer on the surface of the fibers.

In the figures representing 13-93 (Figures 6C, 6D, 7C, 7D), a definite layer cannot be seen on any of the fibers, and the surface is completely clear on about half of the fibers. However, the other half had

multiple tiny granules all around their surface (Figure 6D). The cross-section images also prove that no definite layer formation has occurred (Figures 7C, 7D). The edges of the fibers are fractured possibly due to sanding during the sample preparation.

In figures representing 18-06 (Figures 6E, 6F, 7E, 7F), no definite layer can be seen, and the intact surface is completely clear of deformations on all of the fibers. In the fibers that had grooves, some tiny granules had formed inside the groove. The cross-sectional images (Figures 7E, 7F) also contain no evidence of layer formation. The edges are damaged also on 18-06 fibers possibly due to sanding during the preparation.

In the figures 6G, 6H, 7G and 7H that represent E-glass, no layer formation or surface alteration can be seen on any fiber. The surface is clear in the great majority of fibers. Some unidentified crystals could be seen on separate locations (images not shown), however elemental analysis was not conducted to find out their composition. Similarly, the cross-sectional images present no evidence of layer formation. Additionally, multiple damaged fibers can be seen in the cross-sectional images.

3.3 Energy-Dispersive X-ray Spectroscopy

The data from EDS was translated to show the true SiO_2, Na_2O, and CaO composition of the immersed fibers. The results are shown in Table 2. The 1-06 fibers had 52.4 wt% SiO_2, 6.0 wt% Na_2O and 21.3 wt% CaO. The 13-93 fibers had 70.6 wt% SiO_2, 13.7 wt% Na_2O, and 14.4 wt% CaO. The 18-06 fibers had 71.7 wt% SiO_2, 15.8 wt% Na_2O, and 14.7 wt% CaO. The 1-06 had 2.4 %-unit more silicon and 1.3 %-unit less calcium than the intended glass composition (Tables 1 and 2). The other measured compositions fail to represent the intended compositions. The 18-06 fibers had 6.7 %-unit more silicon and 2.4 %-unit less sodium, and the 13.93 fibers had 18,6 %-units more silicon, 7.7 %-unit more sodium, and 5,6 % unit less calcium than intended (Tables 1 and 2).

Table 2. The true composition of the 1-06, 13-93, and 18-06 BG fibers according to the EDS results. Showing the wt% of the SiO_2, Na_2O, and CaO contents.

	1-06	13-93	18-06
SiO_2	52.4	70.6	71.7
Na_2O	6.0	13.7	15.8
CaO	21.3	14.4	14.7

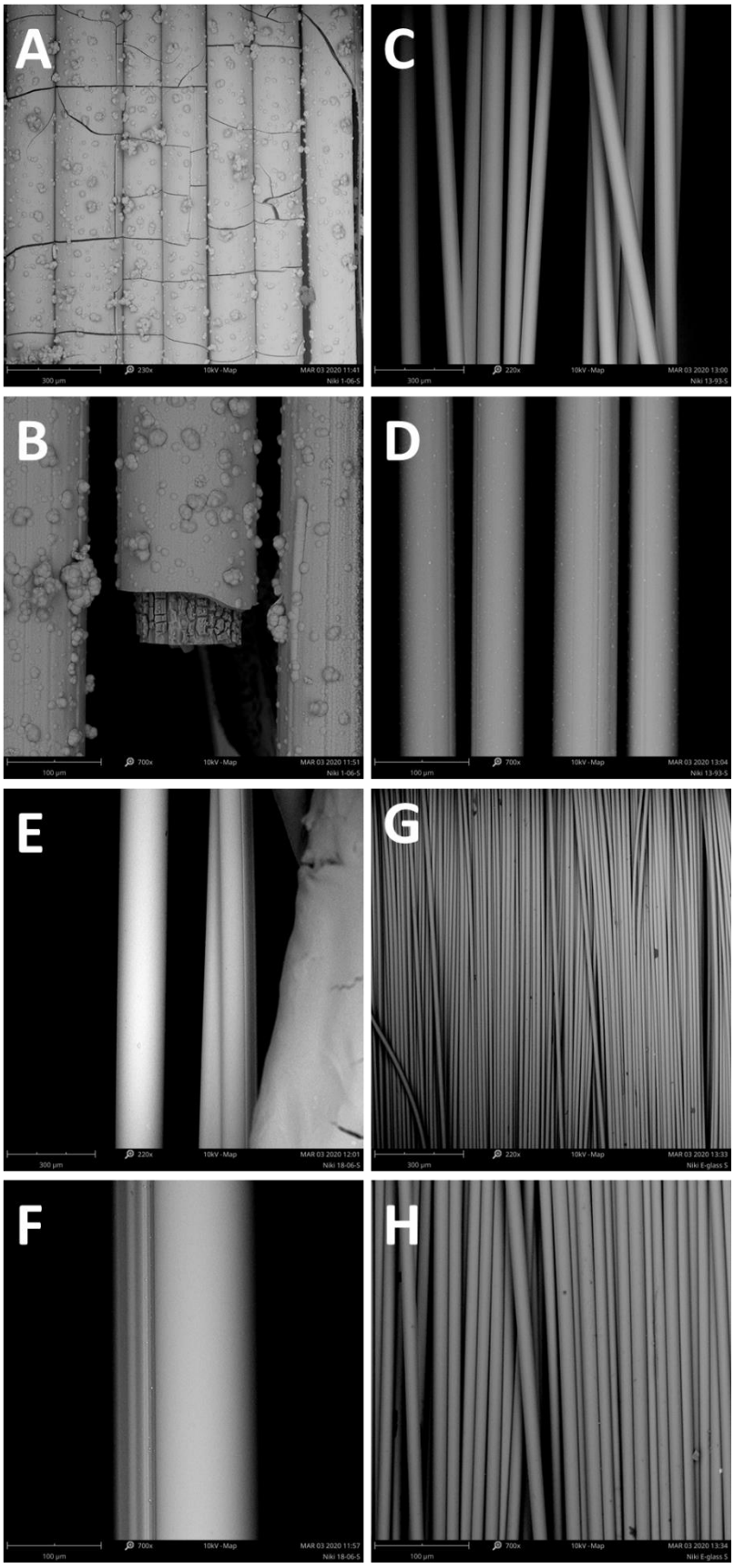

Figure 6. Surface SEM images of the 1-06 (A, B), 13-93 (C, D), 18-06 (E, F) and E-glass (G, H) at 220-230x (A, C, E, G) and 700x (B, D, F, H) magnification.

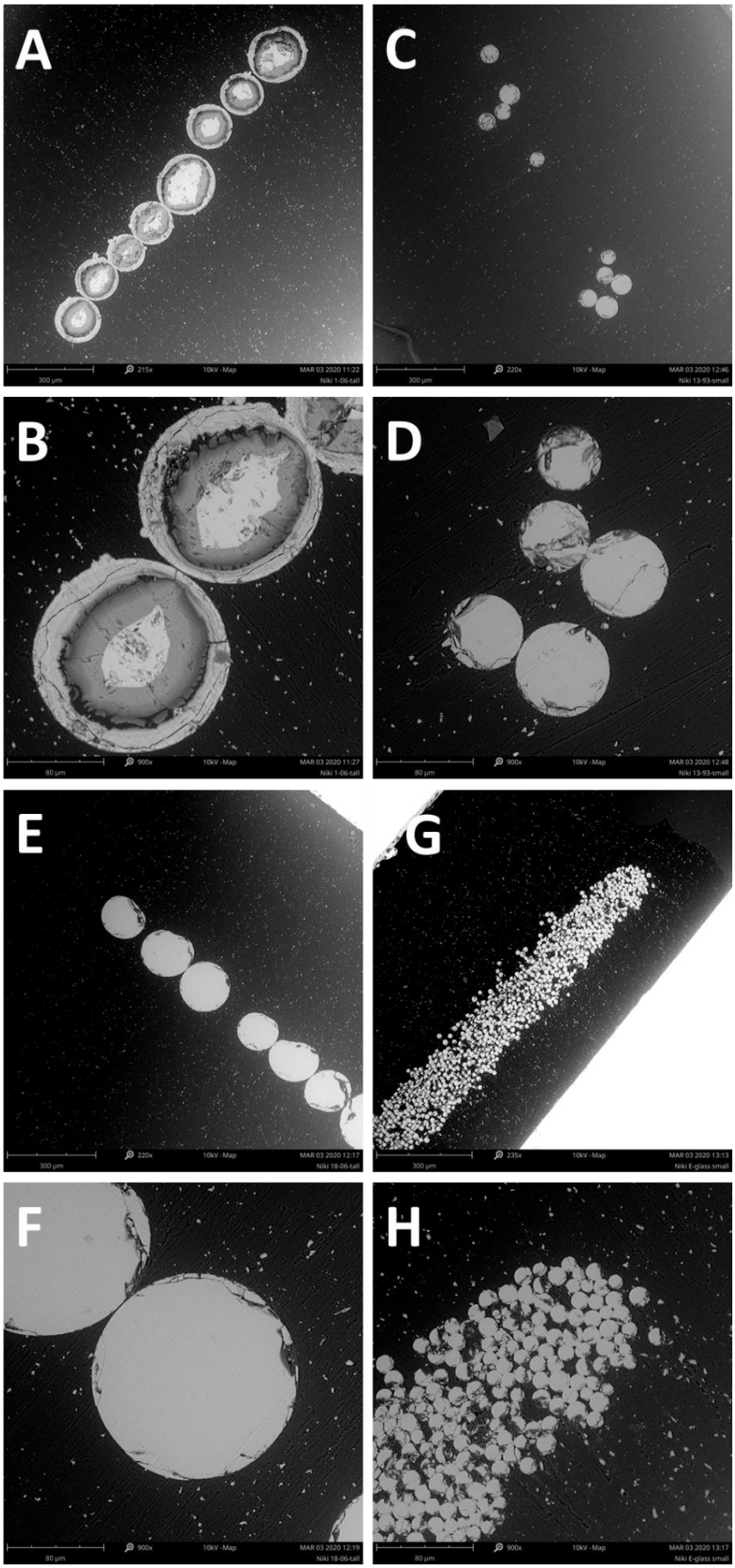

Figure 7. Cross-section SEM images of the 1-06 (A, B), 13-93 (C, D), 18-06 (E, F) and E-glass (G, H) fibers at 215-235x (A, C, E, G) and 900x (B, D, F, H) magnification.

4. Discussion

4.1 Assessment of the Bioactivity Profile and Evaluation of the Results

The purpose of this study was to determine the bioactivity profile for the 1-06, 13-93, and 18-06 bioactive glass fibers and discuss if they are suitable for use as structural parts of a novel biodegradable load-bearing implant.

In study by Vedel *et al.*[47], 13-93 was assessed as medium degree of reactivity with a rapid dissolution of ions, medium reactivity rate (3.2 out of 5, the higher the more reactive) and medium bioactivity number (2.3 out of 3, the higher the more reactive). Establishing this as the control bioactivity profile for a medium BG, establishing the E-glass profile as a control for no bioactivity, and using the data from 13-93 blocks and E-glass fibers, a rough evaluation of the bioactivity profile for the BG fibers can be estimated.

1-06 BG fibers released silicon, sodium, and calcium more slowly than the 13-93 blocks (Figures 2, 4, 5) and the reactivity rate was slower than 13-93 blocks (Figure 3). However, the calcium phosphate layer thickness was not measured from the 13-93 blocks making it challenging to address the relative thickness of the CaP-layer on the 1-06 fibers. Regardless, this would probably place the 1-06 fibers on the lower end of the medium bioactivity profile. 13-93 and 18-06 fibers had similar ion release, reactivity rate and CaP-layer formation behaviour throughout the test, and they followed the same pattern as the negative control (Figures 2-7). Since there was relatively no release of ions, no reactivity from the baseline and no CaP-layer formation, both 13-93 and 18-06 fibers represent nonreactive or really slow bioactivity profile. The bioactive glasses were supposed to represent fast, medium, and slow bioactivity profiles; however, the study results suggested the bioactivity profile was medium for 1-06 fibers and nonreactive for 13-93 and 18-06 fibers.

After immersion to the SBF, the dissolution of the 1-06 fibers can be observed in Figures 2, 4, and 5. Consequently, the formation of the calcium phosphate layer can be observed from the SEM images in the Figures 3, 6, and 7. Also, the decline in phosphate concentration in the SBF analyses indicates that the calcium phosphate is crystallising. However, 13-93 and 18-06 bioactive glass fibers react similarly to the negative control fibers in the dissolution test and SEM analysis and did not display signs of bioactive behaviour. This could mean that the test period was not long enough for the dissolution to be observable and they could both represent the slow bioactivity profile. However, judging by the rapid dissolution of the 13-93 blocks, it is unlikely to be the case indicating that the fiber pulling process affected the glass structure or composition.

The EDS analysis revealed the composition of the immersed fibers and confirmed that the compositions were altered for all of the fibers (Table 2). 1-06 and 18-06 BG fibers have more silicon than intended but the amount of sodium and calcium are within 2%-unit in both glasses (Tables 1 and 2). 13-93 fibers have roughly 6%-unit difference in MO content having more sodium and less calcium than intended (Tables 1 and 2). However, the increase in the silicon content by 18.6 %-unit in the 13-93 fibers and by 6.7 %-unit increase in the 18-06 fibers which already had a high silicon content probably caused them to lose their bioactivity by increasing the NC too much. This probably explains the lack of calcium phosphate layer formation during the SBF immersion for both glasses. According to Hench's early studies[1] the bioactivity starts to decrease fast after the silicon contents pass the 60 wt% point. Additionally, Brink *et al.* tested a variety of bioactive glasses to find out the limits for the BG composition, and they came up with the same approximately 60 wt% upper limit for the silicon content.

In regard of using these fibers in an implant design, the 1-06 fibers could probably be used on the surfaces of the implant to act as a highly active interface between the implant and the bone. Since these fibers were 41% transformed into calcium phosphate during the study period, they would dissolve quickly and facilitate better attachment of the implant to the host tissue. Presuming an exponentially decreasing transformation rate, it would take up to around one to one and a half months for the 1-06 fibers to transform completely. This could still be too fast to consider the 1-06 fibers as the main structural component of a load-bearing implant.

The results of this study cannot conclude the speed of degradation or the bioactivity of the 13-93 or the 18-06 fibers, and therefore additional and probably longer studies with the slower types of bioactive glasses would have to be conducted. Also, the mechanical integrity and strength would have to be assessed to determine the usability of these fibers for load bearing applications.

4.2 Fiber Pulling Methodology

The manual fiber pulling process is probably not an ideal method for achieving consistent fiber quality. In this study, the fibers came out in varying thicknesses and the composition had changed significantly from the intended structure. Since the fibers were pulled from the top of the glass melt, it is possible that the fibers only represent the most surficial layer of the melt glass and therefore fail to represent the holistic consistency of the glass due to the glass being phase separated or improperly homogenized[3,9,55]. Furthermore, the surface of the glass melt is also the most susceptible for crystallization[76] and incorporation of impurities or flaws to the fiber structure more easily. The pulled fibers are also very thin, which requires an even distribution of the ions is the glass structure so that the fibers would have the sought composition. However, researchers have been successful in pulling for example 13-93 fibers

with the intended composition using similar manual methods[61,72] implying that there could be an execution error in the present study.

Bioactive glass fibers have been pulled using a spinner since 1990s[77] by pulling the fibers from an orifice on the bottom of the furnace. Marcolongo *et al.*[77] achieved good quality fibers by this method using a fixed temperature during the pulling. Pirhonen *et al.*[76] used a same method for melting and remelting the glass as in this study but they also used a spinner a to collect the fibers on a reel. With a reel, it is possible to pull with a constant speed and collect consistent fibers that have even thicknesses. Furthermore, by with this method it is possible to keep the crucible in the furnace and have the melt glass at a fixed temperature from which the fibers are pulled. By doing this in the present study, the quality of the glass fibers would have probably been improved since by taking the crucible out of the furnace, the glass starts to cool immediately, and it becomes challenging to control the temperature. In the present study, the viscosity of the glass was tested manually and the fibers were pulled with a rod instead of letting then flow through an orifice definitely created more variability to the pulling process.

Interestingly, Brink *et al.* used a different fiber manufacturing method in another study[78]. They had the similar glass production and melting system used in the melt-spinning technique, however instead of a spinner, they used a spinning stainless steel plate on which they poured the melt glass. The diameter of the fibers was controlled by altering the speed at which the plate was spinning. Although they did not mention the exact diameter of the produced fibers, the figures on the article showed really fine gauge fibers definitely in the sub 100 µm scale, probably around few tens of µm in thickness.

Lately, more advanced fiber pulling methods have been created. Researchers have been able to produce fibers from bioactive glasses using a technique called electrospinning[79,80]. This technique is widely utilized in the BG fiber research mainly because it allows the creation of nanoscale fibers and porous BG scaffolds[79–81]. Deliormanli[81,82] was also able to create fibers from the 13-93 using this method. Electrospinning is a technique that utilizes sol-gel type BG and an electrical field. The glass solution is slowly released from a syringe into an electrical field which then pulls the liquid towards a spinning reel. The thin stream of BG solution quickly polymerizes in the air into nanoscale fibers which can be then collected from the reel for further processing. This technique however is not feasible for the production of fibers with larger thicknesses since the liquid stream needs to be light enough to travel in air while being pulled by the electrical field.

Another technique called laser spinning was first introduced in 2009 by Quintero *et al*[83]. Laser spinning utilizes a high energy laser to melt the end of a solid glass block and then using a high-powered gas flow which blows and elongates the melting droplet effectively pulling it into a fiber. As the melting and blowing happens nearly instantaneously, this allows for really rapid fiber pulling. In their study, they demonstrated this technique by pulling 45S5 and 52S4.6 bioactive glasses into fibers and immersed

them in SBF to demonstrate the preservation of bioactivity. And a result, the glasses produced calcium phosphate layers in 5 days. They also used X-ray fluorescence and a magic angle spinning NMR to verify the composition of the fibers, and even thought composition was slightly altered, they had essentially the intended composition. 45S5 is notorious for having a narrow working range and so far researchers have been unable to pull it into fibers without it crystallizing[10,11,46,47,50,74]. According to the author, the nearly instantaneous melting and cooling cycle prevents the glass from crystallizing and preserves the amorphous state. Furthermore, the laser spinning technique yielded nanoscale fibers that remained separated on the reel while being flexible and easily arrangeable for further processing. This makes laser spinning a very feasible fiber pulling technique for especially for bioactive glasses because it allows fibers to be pulled from virtually any BG, also form narrow working range bioactive glasses, while keeping them easily workable.

Learning from these previous studies, using a spinner to pull the fibers at a constant rate and at a fixed controllable temperature seems to be the best method for pulling good quality fibers in non-industrial setting when not in need of nanoscale fibers and unable to acquire complex equipment. Also, adding multiple remelt cycles to the process seem to be the best method for obtaining a more homogenized consistency for the bulk glass[76,77].

4.3 Estimation of Cell Toxicity

In order to create a successful implant, the cell toxicology would also have to be assessed. According to the literature, 13-93 BG fibers are compatible with osteoblasts and are not cytotoxic[82]. 13-93-based products are also approved for in vivo use in the Europe[84]. Cell cultures with 1-06 BG stay viable and induce osteogenesis in adipose stem cells[19,85,86]. However, no studies using 1-06 BG fibers in cell cultures could be found. Similarly, studies using 18-06 BG in any form could not be found in a literature search from Web of Science or PubMed.

In a comparable study, Valerio *et al*. used a high silicon content BG in their cell culturing studies while trying to assess the effects of bioactive materials on the differentiation, proliferation, viability of rat primary culture osteoblasts[87]. They used a 60 m-% SiO_2 and 35 m-% CaO, and 5 m-% P_2O_5 BG that was produced with the sol-gel method. The high silicon content triggered a vacuole formation inside the cell membranes, but the cells remained viable, preserved their natural morphology, had increased proliferation and collagen production, and reached confluence in the culture plate. In the study, they demonstrated that the vacuole formation was because of the high silicon content and that the vacuoles contained 75% more silicon than other parts in the cells. Whether this causes toxicity or systemic issues in vivo remains unanswered, but this gives some evidence that bone cells react well to high silicon concentration from BGs.

In another study, Karpov *et al.*[88] used an even higher silicon content BG glass while assessing the effects of sol-gel glass ceramics to the differentiation and viability of heterogenous mixture of human bone marrow cells, consisting of osteoblasts and osteoclasts among others. The other glass they used was an 80 % SiO_2, 16 % CaO, and 4 % P_2O_4 BG that was produced by the sol-gel method. In contrast so the study by Valerio *et al.,* this glass greatly enhanced osteoblast differentiation in the culture which was demonstrated by marked increase in ALP mRNA accompanied with decreased expression of osteopontin which is a known to inhibit calcification[89]. In this study, no vacuole formation or other cell toxicity issues were reported. On the contrary, the bone cells responded better to the culturing environment in the presence of BG while the culture lacking BG favoured the growth of fibroblasts.

The two aforementioned studies used different cell lines (rat and human) which may contribute to the difference in reaction to BG's ionic dissolution products, and also the combination of different culture mediums cause variance in cell response. Overall, despite the high silicon content, BG does not seem to cause major adverse reactions in the cell cultures implying that they are mostly safe to use with bone cells. However, more detailed research has to be conducted before unambiguous claims can be made.

4.4 Fiber Reinforced Composites

A bioactive implant has to match the modular and flexural properties of natural bone to become successful as a therapeutic device. By themselves, the glass fibers are rigid but have poor elastic properties and load-bearing capabilities[90]. To increase the feasibility of the fibers, they can be combined with synthetic polymer matrices that can be cured into rigid polymers. Together the fibers and the polymer create a composite that can be engineered to match the structural properties of the cortical bone and becoming a more natural bone-like material than the traditional metallic options[66].

Fiber reinforced composites are traditionally made form inert glass fibers and coupling it with thermoplastic or thermoset polymer. Thermoplastic resins, such as polyethylene, polyetheretherketone, or polyacetal, are first melted and the fibers are added to the melt resin. The fibers become embedded to the polymer matrix as the resin polymerizes. This results in the fibers being physically attached to the polymer matrix as they become entrapped during the polymerization. Thermosets in biomaterial science are usually epoxy resins, such as bis-glycidyl-A-dimethacrylate and triethyleneglycoldimethacrylate copolymer. Epoxy resins achieve higher cross-linking of monomers than the thermoplastics and therefore become stiffer but simultaneously more brittle[66]. However, due to the monomer nature of the resin, the fibers can be sized with a silane coupling agent which will chemically bond the fibers to the polymer during the curing. Because of the free radical based polymerization, thermosets have to be cured to achieve more complete polymerization. The curing is

often induced with specific wavelength in the blue scale of light, and in addition to heat, the material can achieve close to perfect polymerization.

The biocompatibility of the traditional FRCs is good. They are built relatively bioinert, so they cause minimal foreign body reactions in the host. The FRC implants are permanent, so the purpose of the FRC implants is to support the healing of injury and afterwards stay as unnoticeable as possible by mimicking the natural properties of the bone. With the thermosets, unpolymerized epoxy monomers are toxic and can cause inflammatory response if the unpolymerized fraction is too high[91,92]. However, when fully polymerized, they have acceptable biocompatibility and minimal cytotoxicity[68].

4.5 Biodegradable FRCs

Biodegradable polymers, such as poly lactic acid (PLA), poly glycolic acid (PGA), or polycaprolactone (PCA), have been clinically used for decades as sutures, and they are generally regarded as biocompatible. And as an added benefit, they dissolve in the body naturally. However, because of their degradative nature, they lose their structural integrity and stiffness quickly in wet conditions[93] making it challenging to design load-bearing implants that would support the injury until the regenerated bone can support the load. Additionally, the mentioned polymers consist of acidic monomers meaning that dissolution products are acidic and lower pH of the local environment, which can cause inflammation and lead to implant failure[94].

However, in practice, the combination of these biodegradable polymers and bioactive glasses would make an ideal composite material. It would be fully biodegradable, osteogenic, osteoconductive, and it would have self-neutralizing dissolution products that counteract the acidity of the polymer with the alkalinity of the BG. The remaining challenges are to design an implant that would be load bearing and also to have customizable degradation rate to help create the optimal healing environment.

One of the first attempts at creating fully biodegradable implants with bioactive glass fibers are from the late 1990s, when Marcolongo *et al.* created bioactive glass fibers from their own composition (52 m-% SiO_2 and 15 m-% CaO, 30 m-% Na_2O, 3 m-% P_2O_5) and combined it with biodegradable sulfone polymer[77]. The implants had sufficient bioactivity in *in vitro* environment but the polysulfone dissolved too quickly for load bearing applications. In their following study[60], Marcolongo *et al.* demonstrated that this composite material formed adequate bone bonding in *in vivo* environment with only one failure out of 36 specimens and without marked fibrous capsule formation or inflammation in the animals. However, this study was designed to measure the bone bonding ability and biocompatibility and not the load bearing capabilities. They also recognised this in their discussion suggesting that the load bearing applications should be further investigated. Although, good bone bonding capability of biodegradable composite had already been established at this point.

In 2010, Alm *et al*. fabricated a composite by weaving a mesh of 1-98 BG and PLGA polymer in 80/20 ratio of PLA to PGA[95]. They implanted the mesh in New Zealand white rabbits to hold an autologous bone graft. All implants bonded with bone with the BG fibers almost completely resorbed in 12 weeks. No reported inflammatory reactions. However, this composite was not evaluated as osteoproductive rather only osteoconductive. While it did promote bone formation and bonding compared to the intact unoperated bone, it was not significantly more than the PLGA mesh without BG. Also, the defects were not critical size so they would heal by themselves over time. In conclusion, biodegradable fully woven composite could probably work in some clinical applications such as fracture or graft supporting scaffold, it probably would not work in applications requiring load bearing capability due to the lack of hard structural elements.

More recently, Kharazi *et al*. produced a partially biodegradable composite bone plate from poly L-lactic acid (PLLA) and 13-93 fibers[96], and it was intended to be used for fracture fixation. The composite was built by compressing two PLLA fiber sheets around silane sized BG fiber sheet with a hot press acquiring a chemical bond between the components and fully polymerized PLLA layers. In the animal tests, bone plates were placed in New Zealand white rabbits and half of the samples were bonded at the 4 week test group (n =15) and 73% were bonded at the 8-week test group (n=15). Moderate inflammation was observed in both groups, however the inflammation score decreased markedly from 0.8 at 4 weeks to 0.33 at 8 weeks at a scale of 0 to 4 with 0 meaning no inflammation and 4 meaning severe inflammation. The positive biological response implies that this composite retains its bioactivity, and the inflammatory and fibrous capsule formation are mostly very mild or non-existent. They also tested the rate of degradation which remained constant throughout the testing period. No sign of exponential degradation was present. According to the study title, the implant was intended to be load bearing, however, the study was lacking the mechanical tests to demonstrate the load bearing capability. They claimed that the load was supposed to transfer on new grown bone after one month of implantation, which very well might be true in the case of fracture fixation.

In another recent study, Wu *et al.* tested a novel commercial BG/poly L-D-lactic acid (PLDLA) composite plates for their biocompatibility and bone regenerative capabilities[97]. The composite was sold by a Finnish Arctic Biomaterials Oy, however they did not disclose the composition of the used BG. On the company website, the composite appears to be a mixture of a thermoplastic polymer and glass fibers in a random alignment which has been extruded or injection moulded into shape[98]. They claim to be using some proprietary manufacturing techniques called Automated Fiber Placement which allows them to computerize the optimal fiber placement, and they claim to be the first company providing load bearing biodegradable composites for medical use. In the published study, Wu *et al.* had the composite re-processed at a Chinese company into small pins that were inserted into bone and muscle tissues of Beagle dogs[97]. The pins had a fiber fraction of 27,5 % and longitudinal parallel fiber. In the two year

study, the composite demonstrated excellent biocompatibility, and bone bonding and osteoproductive capability. The composite performed superiorly to the plain PLDLA polymer in regard of tissue contact, angiogenesis, and bone regeneration for the first year.

In another study by the same research group, they assessed the mechanical and degradative properties of the same PLDLA/BG composite over the same period of time[99]. Also in this study, the composite material performed superiorly to the plain PLDLA in terms of strength retention and degradation rate for the first half of a year. The composite demonstrated superior mechanical characteristics for the first 52 weeks and remained relatively stable for the first 26 weeks which according to the authors would be enough for most clinical load bearing applications. After 52 weeks, the composite started to degrade faster possibly due to number of interconnected pores left by the degraded BG fibers. All in all, this composite material is so far the most promising option for clinical load bearing applications, and these long term *in vivo* studies support the clinical relevance.

4.6 Designing Biodegradable Implants

The material choice is the first step in creating a biodegradable composite. Based on the studies presented in the previous chapters, mixture of both L and D isomers of poly lactic acid and poly glycolic acid seem to be the most utilized materials for the polymer. They offer great processing capabilities and a possibility to freely engineer the mechanical and degradative properties while being largely biocompatible. They retain their shape and mechanical strength for a long time making them feasible also for supporting the regeneration of large defects. For example, PLDLA (L/D ratio of 80/20) retains its shape for over 2 years and their mechanical strength relatively stable for over a year before it starts to degrade more rapidly at around one and a half to two years[97,99].

The choice for BG fibers is little more complicated, since the BG has to have large working range and be sufficiently bioactive, which have been proven to be at the opposite ends of the compositional range[73]. In regard of the fibers used in the present study, more studies have to conducted on 1-06 and 18-06 fibers to find out their eligibility for implant construction. However, degradation and mechanical studies have been conducted on 13-93 fibers by other researchers. According to the study by Pirhonen *et al.*, the 13-93 fibers steadily lose their structural integrity during the first 5 weeks, but maintain nearly constant mechanical strength afterwards for about 40 weeks[72]. They speculated that this phenomenon was because of the calcium phosphate layer reached a critical level of thickness at which it starts to slow down the further degradation of the fibers by inhibiting the water penetration. While this is an interesting discovery, this kind of change in the dissolution characteristics necessitates further studies regarding the changes in the long term degradation rate and physical properties based on the composition of the BG fibers both *in vivo* and *in vitro.* It would be helpful to find out the exact time points

for certain BG fibers where they reach the limits of load bearing capability and flexural strengths. It is also interesting to know if the starting point of the slower degradation could be controlled, and how much of the original strength can be maintained at this state.

While there are studies that have discovered the compositional range for BG that is both workable and bioactive[8,54,55,73], there is a lack of comprehensive studies addressing the compositional dependence of both components of composite fibers on their mechanical behaviour and bioactivity in aqueous conditions. Since the behaviour of the separate components can be vastly different on their own than when they are used together, the compositional dependence of the composite components is vital for implant design. For example, the acidic degradation products of the polymer can have a slowing effect on the degradation of the BG fibers and consequently affect the bioactivity and antimicrobial properties of the glass.

A study from Lehtonen *et al.* tries to explain the change in mechanical characteristics of bioresorbable PLA/BG composite fibers in SBF[100]. They used a static PLA to BG ratio and three different compositions for the BG fibers for the tests. Also in their study, they found out that all of the composite fibers reach a stage where the degradation slows down but also that the steady state was directly related to the complete loss of the mechanical strength. However, the strongest composite they tested retained suitable flexural strength for load bearing capability for approximately 8-10 weeks which is plenty for clinical bone reconstruction and fixation purposes[66].

Another point worth further studying could be the creation of hybrid fiber structures. The 13-93 BG fibers could be bundled together with the 1-06 fibers and the reactivity of the implant surface could be more accurately engineered without having to invent a novel BG. A hybrid fiber bundle would have the characteristics from both fibers and it would allow for easy modification to achieve the desired properties by changing the ratios between the glasses. By using the two types of fibers together, it could be possible to control the speed of the bonding and surface reactivity. This way a more dynamic range of dissolution and reactivity characteristics could be acquired form the same materials.

However, in the end, the material choices is only one part in designing the structural properties for the final implant. The volume fraction, directionality, and thickness of the fibers and also the implant design affect the structural rigidity, flexural properties, and durability[49]. In a study by Pirhonen *et al.,* the volume fraction of the fibers affected the flexural strength and modulus of a PLA/13-93 BG composite significantly, and only the samples that had fiber content of 30% or more reached the strength of cortical bone[101]. The directional alignment of the fibers also has a big impact on the tensional strength of the implant. Unidirectional fibers increase the tensile strength while bidirectional alignment increase the flexural stiffness of the implant. A combination of unidirectional rods and bidirectional fibers in some areas can be used to further improve the stability of the implant under torsional and compressive

stresses[16,66]. The implant design allows the engineering of multiple properties by creating different shapes or surface structures to the final product. Different grooves, threading, surface coating, such as protein or BG coating, or surface roughening can be added to facilitate better fixation to the bone or accommodate to the natural shape of the bone structure[49,102,103]. By adding areas of different fiber alignment or volume fraction, the structural properties of the implant can be fine-tuned for each individual patient to create more personalized treatment and possibly reduce the risk of implant failure.

Additionally, the synthetic biopolymers provide another beneficial feature for designing implants as they can be transformed into filaments and utilized in three-dimensional (3D) modelling systems such as fused deposition modelling (FDM). FDM allows the engineering of controllable porosity, complex micrometre-scale shapes, and easily reproducible consistent components, but it also enables creation of hybrid multi-layer structures from different polymers. FDM allows more freedom for the implant design and structural property engineering. For example, early 2000 Zein *et al*. designed porous scaffolds from PCL using the FDM technique[104]. They demonstrated the possibilities of FDM as a scaffold engineering technique by producing scaffold of controlled porosity and strength equivalent to typical porous scaffolds. In the follow up study, they proceeded to demonstrate successful cell attachment and proliferation of human fibroblast and osteoblast-like cells in *in vitro* environment[105]. In this study, the cells were able to proliferate and remained viable displaying good biocompatibility and safety of the scaffolds[105]. Following the positive results from the previous study, they attached primary human osteoprogenitor cells to the scaffolds and demonstrated the bone-bonding capability of the scaffolds *in vivo* in Balb C nude mice[106].

In the present study, FDM was utilized in the specimen scaffold production and the possibility of adding glass fibers to the printed structure was demonstrated. PLA was used as the polymer filament, and by first printing a base and then adding the fibers on top, it was possible to integrate the fibers to the structure when proceeding the print. The fibers would be sandwiched between the layers and attached to the structure. The overall thickness and also the variability of thicknesses of the manually pulled BG fibers caused some challenges in the attachment to the scaffold, but when using the much thinner E-glass fibers, almost complete integration of the fibers was achieved. However, the attachment achieved by this method is completely mechanical and without a chemical connection. The possibility of sizing the fibers with a coupling agent to also reach a chemical bond between the fibers and the PLA should be further investigated, since sizing has been shown to increase the mechanical properties of BG/PLA composites[100].

Another fully computerized scaffolding method that could be utilized is embroidery[69]. With embroidery, more advanced and complex fiber alignment can be achieved. Also, polymer and BG fibers could be intertwined more closely for homogenous structure. Solely woven meshes are flexible and stretchable, and if load bearing is needed, the mesh could be coated with varying polymers to achieve rigidity.

Embroidery has been successfully utilized with biodegradable polymers and BG coatings[70,71,107], however BG fibers have yet to be used with this technique. Embroidery provides an attractive option for implant production, since it is fast, computerized, reproducible, and versatile technique which is still largely underutilized.

5. Conclusions

Glass fibers were pulled from three bioactive glass compositions to evaluate their bioactivity and usability in a novel load bearing composite material. As a result, the 1-06 fibers were considered to have medium bioactivity but the 13-93 and the 18-06 fibers were nonreactive in the SBF testing. However, the glass compositions of the fibers were heavily altered from the intended composition probably due to the original glass being phase separated or improperly homogenized, or the fiber pulling methodology affected the original composition. Therefore, the evaluation of the usability of these fibers for designing implants on the basis of this study remains inconclusive. Nevertheless, the important characteristics, properties, and material choices for a proper load bearing implant design were identified through literature search. Both isomers of PLA and PGL were evaluated to be suitable for the polymer component, and at least 13-93 is suitable for bioactive glass fiber component. However, a lack of proper studies assessing the compositional dependence of the different components on the mechanical and bioactive properties of biodegradable composites limited the ability to make more accurate estimations of the optimal materials. The optimal compositional range for PLA D/L ratio, PLA to PGA ratio, BG fiber fraction, fiber alignment, and BG composition in a composite material is not known. This necessitates further studies to find out the optimal parameters for load bearing composites.

6. Acknowledgements

I acknowledge Niko Moritz and Yulia Kulkova for enabling this Master's thesis, and giving valuable guidance and feedback during the project.

I acknowledge Jaana Paananen for her help with the glass production and fiber pulling.

I acknowledge Peter Uppstu for his help with the ICP-OES.

I acknowledge Artem Plyushnin for his help and support during the sample preparation and SEM/EDS analyses.

I acknowledge Kaveh Nik Jamal for his help during the SEM/EDS analyses.

6. List of abbreviations

BG = bioactive glass

BO = Bridging oxygen

CaP = Calcium phosphate

ECM = Extracellular matrix

ECF = Extracellular fluid

EDS = Energy-dispersive X-ray spectroscopy

FRC = Fiber reinforced composite

HA = hydroxyapatite

MO = Modifier oxide

NBO = Non-bridging oxygen

SBF = Simulated body fluid

SEM = Scanning electron microscopy

7. References

1. Hench LL. The story of Bioglass®. *J Mater Sci Mater Med*. 2006;17(11):967-978. doi:10.1007/s10856-006-0432-z

2. Hench LL, Paschall HA. Direct chemical bond of bioactive glass-ceramic materials to bone and muscle. *J Biomed Mater Res*. 1973;7(3):25-42. doi:10.1002/jbm.820070304

3. Elgayar I, Aliev AE, Boccaccini AR, Hill RG. Structural analysis of bioactive glasses. *J Non Cryst Solids*. 2005;351(2):173-183. doi:10.1016/j.jnoncrysol.2004.07.067

4. Brauer DS. Bioactive glasses - Structure and properties. *Angew Chemie - Int Ed*. 2015;54(14):4160-4181. doi:10.1002/anie.201405310

5. Jugdaohsingh R. Silicon and bone health. In: *Journal of Nutrition, Health and Aging*. Vol 11. ; 2007:99-110.

6. Arcos D, Greenspan DC, Vallet-Regí M. A new quantitative method to evaluate the in vitro bioactivity of melt and sol-gel-derived silicate glasses. *J Biomed Mater Res - Part A*. 2003;65(3):344-351. doi:10.1002/jbm.a.10503

7. Tulyaganov D, Abdukayumov K, Ruzimuradov O, Hojamberdiev M, Ionescu E, Riedel R. Effect of alumina incorporation on the surface mineralization and degradation of a bioactive glass (CaO-MgO-SiO2-Na2O-P2O5-CaF2)-glycerol paste. *Materials (Basel)*. 2017;10(11). doi:10.3390/ma10111324

8. Mathew R, Stevensson B, Tilocca A, Edén M. Toward a rational design of bioactive glasses with optimal structural features: Composition-structure correlations unveiled by solid-state NMR and MD simulations. *J Phys Chem B*. 2014;118(3):833-844. doi:10.1021/jp409652k

9. Tilocca A, Cormack AN, De Leeuw NH. The structure of bioactive silicate glasses: New insight from molecular dynamics simulations. *Chem Mater*. 2007;19(1):95-103. doi:10.1021/cm061631g

10. Arstila H, Zhang D, Vedel E, Hupa L, Ylänen HO, Hupa M. Bioactive Glass Compositions Suitable for Repeated Heat-Treatments. *Key Eng Mater*. 2005;284-286:925-928. doi:10.4028/www.scientific.net/kem.284-286.925

11. Zhang D, Vedel E, Hupa L. Predicting physical and chemical properties of bioactive glasses from chemical composition. Part 3: In vitro reactivity | Sandy Zhang - Academia.edu. *Glas Technol - Eur J Glas Sci Technol*. 2009;50:1-8.

12. Hench LL. Bioceramics: From Concept to Clinic. *J Am Ceram Soc*. 1991;74(7):1487-1510.

doi:10.1111/j.1151-2916.1991.tb07132.x

13. Stevensson B, Mathew R, Edén M. Assessing the phosphate distribution in bioactive phosphosilicate glasses by 31P solid-state NMR and molecular dynamics simulations. *J Phys Chem B*. 2014;118(29):8863-8876. doi:10.1021/jp504601c

14. Ning C, Zhou L, Tan G. Fourth-generation biomedical materials. *Mater Today*. 2016;19(1):2-3. doi:10.1016/j.mattod.2015.11.005

15. Kankare J, Lindfors NC. Reconstruction of Vertebral Bone Defects using an Expandable Replacement Device and Bioactive Glass S53P4 in the Treatment of Vertebral Osteomyelitis: Three Patients and Three Pathogens. *Scand J Surg*. 2016;105(4):248-253. doi:10.1177/1457496915626834

16. Vallittu PK. Bioactive glass-containing cranial implants: an overview. *J Mater Sci*. 2017;52(15):8772-8784. doi:10.1007/s10853-017-0888-x

17. Tuusa SM-R, Peltola MJ, Tirri T, Lassila LVJ, Vallittu PK. Frontal bone defect repair with experimental glass-fiber-reinforced composite with bioactive glass granule coating. *J Biomed Mater Res - Part B Appl Biomater*. 2007;82(1):149-155. doi:10.1002/jbm.b.30716

18. Lindfors N, Geurts J, Drago L, et al. Antibacterial bioactive glass S53P4 for chronic bone infections – A multinational study. In: *Advances in Experimental Medicine and Biology*. Vol 971. Springer New York LLC; 2017:81-92. doi:10.1007/5584_2016_156

19. Ojansivu M, Wang X, Hyväri L, et al. Bioactive glass induced osteogenic differentiation of human adipose stem cells is dependent on cell attachment mechanism and mitogen-activated protein kinases. *Eur Cells Mater*. 2018;35:53-71. doi:10.22203/eCM.v035a05

20. Hoppe A, Güldal NS, Boccaccini AR. A review of the biological response to ionic dissolution products from bioactive glasses and glass-ceramics. *Biomaterials*. 2011;32(11):2757-2774. doi:10.1016/j.biomaterials.2011.01.004

21. Hench LL. Genetic design of bioactive glass. *J Eur Ceram Soc*. 2009;29(7):1257-1265. doi:10.1016/j.jeurceramsoc.2008.08.002

22. Xynos ID, Edgar AJ, Buttery LDK, Hench LL, Polak JM. Gene-expression profiling of human osteoblasts following treatment with the ionic products of Bioglass 45S5 dissolution. *J Biomed Mater Res*. 2001;55(2):151-157. doi:10.1002/1097-4636(200105)55:2<151::AID-JBM1001>3.0.CO;2-D

23. Xynos ID, Hukkanen MVJ, Batten JJ, Buttery LD, Hench LL, Polak JM. Bioglass ®45S5 stimulates

osteoblast turnover and enhances bone formation in vitro: Implications and applications for bone tissue engineering. *Calcif Tissue Int*. 2000;67(4):321-329. doi:10.1007/s002230001134

24. Maeno S, Niki Y, Matsumoto H, et al. The effect of calcium ion concentration on osteoblast viability, proliferation and differentiation in monolayer and 3D culture. *Biomaterials*. 2005;26(23):4847-4855. doi:10.1016/j.biomaterials.2005.01.006

25. Marie PJ. The calcium-sensing receptor in bone cells: A potential therapeutic target in osteoporosis. *Bone*. 2010;46(3):571-576. doi:10.1016/j.bone.2009.07.082

26. Xynos ID, Edgar AJ, Buttery LDK, Hench LL, Polak JM. Ionic products of bioactive glass dissolution increase proliferation of human osteoblasts and induce insulin-like growth factor II mRNA expression and protein synthesis. *Biochem Biophys Res Commun*. 2000;276(2):461-465. doi:10.1006/bbrc.2000.3503

27. Narita H, Itoh S, Imazato S, Yoshitake F, Ebisu S. An explanation of the mineralization mechanism in osteoblasts induced by calcium hydroxide. *Acta Biomater*. 2010;6(2):586-590. doi:10.1016/j.actbio.2009.08.005

28. Dvorak MM, Siddiqua A, Ward DT, et al. Physiological changes in extracellular calcium concentration directly control osteoblast function in the absence of calciotropic hormones. *Proc Natl Acad Sci U S A*. 2004;101(14):5140-5145. doi:10.1073/pnas.0306141101

29. Yamaguchi T, Chattopadhyay N, Kifor O, et al. Expression of extracellular calcium-sensing receptor in human osteoblastic MG-63 cell line. *Am J Physiol - Cell Physiol*. 2001;280(2 49-2). doi:10.1152/ajpcell.2001.280.2.c382

30. Zou S, Ireland D, Brooks RA, Rushton N, Best S. The effects of silicate ions on human osteoblast adhesion, proliferation, and differentiation. *J Biomed Mater Res - Part B Appl Biomater*. 2009;90 B(1):123-130. doi:10.1002/jbm.b.31262

31. Reffitt DM, Ogston N, Jugdaohsingh R, et al. Orthosilicic acid stimulates collagen type 1 synthesis and osteoblastic differentiation in human osteoblast-like cells in vitro. *Bone*. 2003;32(2):127-135. doi:10.1016/S8756-3282(02)00950-X

32. Mladenović Ž, Johansson A, Willman B, Shahabi K, Björn E, Ransjö M. Soluble silica inhibits osteoclast formation and bone resorption in vitro. *Acta Biomater*. 2014;10(1):406-418. doi:10.1016/j.actbio.2013.08.039

33. Wiens M, Wang X, Schröder HC, et al. The role of biosilica in the osteoprotegerin/RANKL ratio in human osteoblast-like cells. *Biomaterials*. 2010;31(30):7716-7725. doi:10.1016/j.biomaterials.2010.07.002

34. Julien M, Khoshniat S, Lacreusette A, et al. Phosphate-dependent regulation of MGP in osteoblasts: Role of ERK1/2 and Fra-1. *J Bone Miner Res*. 2009;24(11):1856-1868. doi:10.1359/jbmr.090508

35. Munukka E, Leppäranta O, Korkeamäki M, et al. Bactericidal effects of bioactive glasses on clinically important aerobic bacteria. *J Mater Sci Mater Med*. 2008;19(1):27-32. doi:10.1007/s10856-007-3143-1

36. Drago L, De Vecchi E, Bortolin M, Toscano M, Mattina R, Romanò CL. Antimicrobial activity and resistance selection of different bioglass S53P4 formulations against multidrug resistant strains. *Future Microbiol*. 2015;10(8):1293-1299. doi:10.2217/FMB.15.57

37. Drago L, Vassena C, Fenu S, et al. In vitro antibiofilm activity of bioactive glass S53P4. *Future Microbiol*. 2014;9(5):593-601. doi:10.2217/fmb.14.20

38. Stoor P, Soderling E, Salonen JI. Antibacterial effects of a bioactive glass paste on oral microorganisms. *Acta Odontol Scand*. 1998;56(3):161-165. doi:10.1080/000163598422901

39. Zhang D, Leppäranta O, Munukka E, et al. Antibacterial effects and dissolution behavior of six bioactive glasses. *J Biomed Mater Res - Part A*. 2010;93(2):475-483. doi:10.1002/jbm.a.32564

40. Bortolin M, Vecchi E De, Romano CL, Toscano M, Mattina R, Drago L. Antibiofilm agents against mdr bacterial strains: Is bioactive glass bag-s53p4 also effective? *J Antimicrob Chemother*. 2016;71(1):123-127. doi:10.1093/jac/dkv327

41. McConoughey SJ, Howlin R, Granger JF, et al. Biofilms in periprosthetic orthopedic infections. *Future Microbiol*. 2014;9(8):987-1007. doi:10.2217/fmb.14.64

42. Neut D, Van Der Mei HC, Bulstra SK, Busscher HJ. The role of small-colony variants in failure to diagnose and treat biofilm infections in orthopedics. *Acta Orthop*. 2007;78(3):299-308. doi:10.1080/17453670710013843

43. Detsch R, Stoor P, Grünewald A, Roether JA, Lindfors NC, Boccaccini AR. Increase in VEGF secretion from human fibroblast cells by bioactive glass S53P4 to stimulate angiogenesis in bone. *J Biomed Mater Res - Part A*. 2014;102(11):4055-4061. doi:10.1002/jbm.a.35069

44. Lindfors NC, Hyvönen P, Nyyssönen M, et al. Bioactive glass S53P4 as bone graft substitute in treatment of osteomyelitis. *Bone*. 2010;47(2):212-218. doi:10.1016/j.bone.2010.05.030

45. Bose S, Roy M, Bandyopadhyay A. Recent advances in bone tissue engineering scaffolds. *Trends Biotechnol*. 2012;30(10):546-554. doi:10.1016/j.tibtech.2012.07.005

46. Arstila H, Vedel E, Hupa L, Hupa M. Factors affecting crystallization of bioactive glasses. *J Eur Ceram Soc*. 2007;27(2-3):1543-1546. doi:10.1016/j.jeurceramsoc.2006.04.017

47. Vedel E, Zhang D, Arstila H, Hupa L, Hupa M. Predicting physical and chemical properties of bioactive glasses from chemical composition. Part 4: Tailoring compositions with desiredproperties. *Glas Technol Eur J Glas Sci Technol Part A*. 2009;50(1):9-16.

48. Hench LL, Xynos ID, Polak JM. Bioactive glasses for in situ tissue regeneration. *J Biomater Sci Polym Ed*. 2004;15(4):543-562. doi:10.1163/156856204323005352

49. Albrektsson T, Brånemark PI, Hansson HA, Lindström J. Osseointegrated titanium implants: Requirements for ensuring a long-lasting, direct bone-to-implant anchorage in man. *Acta Orthop*. 1981;52(2):155-170. doi:10.3109/17453678108991776

50. Arstila H, Hupa L, Karlsson KH, Hupa M. Influence of heat treatment on crystallization of bioactive glasses. *J Non Cryst Solids*. 2008;354(2-9):722-728. doi:10.1016/j.jnoncrysol.2007.06.092

51. Lotfibakhshaiesh N, Brauer DS, Hill RG. Bioactive glass engineered coatings for Ti6Al4V alloys: Influence of strontium substitution for calcium on sintering behaviour. In: *Journal of Non-Crystalline Solids*. Vol 356. ; 2010:2583-2590. doi:10.1016/j.jnoncrysol.2010.05.017

52. Hahner J, Hinüber C, Breier A, Siebert T, Brünig H, Heinrich G. Adjusting the mechanical behavior of embroidered scaffolds to lapin anterior cruciate ligaments by varying the thread materials. *Text Res J*. 2015;85(14):1431-1444. doi:10.1177/0040517514566107

53. Brauer DS, Wilson RM, Kasuga T. Multicomponent phosphate invert glasses with improved processing. *J Non Cryst Solids*. 2012;358(14):1720-1723. doi:10.1016/j.jnoncrysol.2012.04.027

54. Brink M. The influence of alkali and alkaline earths on the working range for bioactive glasses. *J Biomed Mater Res*. 1997;36(1):109-117. doi:10.1002/(SICI)1097-4636(199707)36:1<109::AID-JBM13>3.0.CO;2-D

55. Tylkowski M, Brauer DS. Mixed alkali effects in Bioglass® 45S5. *J Non Cryst Solids*. 2013;376:175-181. doi:10.1016/j.jnoncrysol.2013.05.039

56. Blaeß C, Müller R, Poologasundarampillai G, Brauer DS. Sintering and concomitant crystallization of bioactive glasses. *Int J Appl Glas Sci*. 2019;10(4):449-462. doi:10.1111/ijag.13477

57. Watts SJ, Hill RG, O'Donnell MD, Law R V. Influence of magnesia on the structure and properties of bioactive glasses. *J Non Cryst Solids*. 2010;356(9-10):517-524. doi:10.1016/j.jnoncrysol.2009.04.074

58. Fredholm YC, Karpukhina N, Law R V., Hill RG. Strontium containing bioactive glasses: Glass structure and physical properties. In: *Journal of Non-Crystalline Solids*. Vol 356. North-Holland; 2010:2546-2551. doi:10.1016/j.jnoncrysol.2010.06.078

59. Fujikura K, Karpukhina N, Kasuga T, Brauer DS, Hill RG, Law R V. Influence of strontium substitution on structure and crystallisation of Bioglass® 45S5. *J Mater Chem*. 2012;22(15):7395-7402. doi:10.1039/c2jm14674f

60. Marcolongo M, Ducheyne P, Garino J, Schepers E. Bioactive glass fiber/polymeric composites bond to bone tissue. *J Biomed Mater Res*. 1998;39(1):161-170. doi:10.1002/(SICI)1097-4636(199801)39:1<161::AID-JBM18>3.0.CO;2-I

61. Brown RF, Day DE, Day TE, Jung S, Rahaman MN, Fu Q. Growth and differentiation of osteoblastic cells on 13-93 bioactive glass fibers and scaffolds. *Acta Biomater*. 2008;4(2):387-396. doi:10.1016/j.actbio.2007.07.006

62. Bunting S, Di Silvio L, Deb S, Hall S, Standring S. Bioresorbable glass fibres facilitate peripheral nerve regeneration. *J Hand Surg Am*. 2005;30(3):242-247. doi:10.1016/j.jhsb.2004.11.003

63. Minatoya T, Furusawa T, Sato M, Matsushima Y, Unuma H. Bioactive glass cloth that promotes new bone formation. In: *Key Engineering Materials*. Vol 529-530. ; 2013:266-269. doi:10.4028/www.scientific.net/KEM.529-530.266

64. Zhao S, Li L, Wang H, et al. Wound dressings composed of copper-doped borate bioactive glass microfibers stimulate angiogenesis and heal full-thickness skin defects in a rodent model. *Biomaterials*. 2015;53:379-391. doi:10.1016/j.biomaterials.2015.02.112

65. Hong Y, Chen X, Jing X, Fan H, Gu Z, Zhang X. Fabrication and drug delivery of ultrathin mesoporous bioactive glass hollow fibers. *Adv Funct Mater*. 2010;20(9):1503-1510. doi:10.1002/adfm.200901627

66. Vallittu PK, Närhi TO, Hupa L. Fiber glass-bioactive glass composite for bone replacing and bone anchoring implants. *Dent Mater*. 2015;31(4):371-381. doi:10.1016/j.dental.2015.01.003

67. Posti JP, Piitulainen JM, Hupa L, et al. A glass fiber-reinforced composite - bioactive glass cranioplasty implant: A case study of an early development stage implant removed due to a late infection. *J Mech Behav Biomed Mater*. 2016;55:191-200. doi:10.1016/j.jmbbm.2015.10.030

68. Ballo AM, Akca EA, Ozen T, Lassila L, Vallittu PK, Närhi TO. Bone tissue responses to glass fiber-reinforced composite implants - A histomorphometric study. *Clin Oral Implants Res*. 2009;20(6):608-615. doi:10.1111/j.1600-0501.2008.01700.x

69. Breier A. Embroidery technology for hard-tissue scaffolds. In: Todd B, ed. *Biomedical Textiles for Orthopaedic and Surgical Applications: Fundamentals, Application and Tissue Engineering*. Cambridge: Woodhead Publishing; 2015:23-43.

70. Hoyer M, Drechsel N, Meyer M, et al. Embroidered polymer-collagen hybrid scaffold variants for ligament tissue engineering. *Mater Sci Eng C*. 2014;43:290-299. doi:10.1016/j.msec.2014.07.010

71. Rentsch B, Hofmann A, Breier A, Rentsch C, Scharnweber D. Embroidered and surface modified polycaprolactone-co-lactide scaffolds as bone substitute: In vitro characterization. *Ann Biomed Eng*. 2009;37(10):2118-2128. doi:10.1007/s10439-009-9731-0

72. Pirhonen E, Niiranen H, Niemelä T, Brink M, Törmälä P. Manufacturing, mechanical characterization, and in vitro performance of bioactive glass 13-93 fibers. *J Biomed Mater Res - Part B Appl Biomater*. 2006;77(2):227-233. doi:10.1002/jbm.b.30429

73. Brink M, Turunen T, Happonen RP, Yli-Urpo A. Compositional dependence of bioactivity of glasses in the system Na2O- K2O-MgO-Cao-B2O3-P2O5-SiO2. *J Biomed Mater Res*. 1997;37(1):114-121. doi:10.1002/(SICI)1097-4636(199710)37:1<114::AID-JBM14>3.0.CO;2-G

74. Zhang D, Arstila H, Vedel E, Ylänen H, Hupa L, Hupa M. In vitro behavior of fiber bundles and particles of bioactive glasses. In: Daculsi G, Layrolle P, eds. *Key Engineering Materials*. Vol 361-363 I. Trans Tech Publications, Ltd.; 2008:223-228. doi:10.4028/www.scientific.net/kem.361-363.225

75. Kokubo T, Takadama H. How useful is SBF in predicting in vivo bone bioactivity? *Biomaterials*. 2006;27(15):2907-2915. doi:10.1016/j.biomaterials.2006.01.017

76. Pirhonen E, Moimas L, Brink M. Mechanical properties of bioactive glass 9-93 fibres. *Acta Biomater*. 2006;2(1):103-107. doi:10.1016/j.actbio.2005.08.008

77. Marcolongo M, Ducheyne P, LaCourse WC. Surface reaction layer formation in vitro on a bioactive glass fiber/polymeric composite. *J Biomed Mater Res*. 1997;37(3):440-448. doi:10.1002/(SICI)1097-4636(19971205)37:3<440::AID-JBM15>3.0.CO;2-F

78. Brink M, Laine P, Narva K, Yli-Urpo A. Implantation of bioactive and inert glass fibres in rats—Soft tissue response and short-term reactions of the glass. In: Sedel L, Ray C, eds. *Bioceramics*. Elsevier Ltd; 1997:61-64. doi:10.1016/b978-008042692-1/50015-7

79. Xie J, Blough ER, Wang CH. Submicron bioactive glass tubes for bone tissue engineering. *Acta Biomater*. 2012;8(2):811-819. doi:10.1016/j.actbio.2011.09.009

80. Hong Y, Chen X, Jing X, et al. Preparation, bioactivity, and drug release of hierarchical nanoporous bioactive glass ultrathin fibers. *Adv Mater*. 2010;22(6):754-758. doi:10.1002/adma.200901656

81. Deliormanlı AM. Electrospun cerium and gallium-containing silicate based 13-93 bioactive glass fibers for biomedical applications. *Ceram Int*. 2016;42(1):897-906.

doi:10.1016/j.ceramint.2015.09.016

82. Deliormanli AM. Preparation, in vitro mineralization and osteoblast cell response of electrospun 13-93 bioactive glass nanofibers. *Mater Sci Eng C*. 2015;53:262-271. doi:10.1016/j.msec.2015.04.037

83. Quintero F, Pou J, Comesaña R, et al. Laser spinning of bioactive glass nanofibers. *Adv Funct Mater*. 2009;19(19):3084-3090. doi:10.1002/adfm.200801922

84. Rahaman MN, Day DE, Sonny Bal B, et al. Bioactive glass in tissue engineering. *Acta Biomater*. 2011;7(6):2355-2373. doi:10.1016/j.actbio.2011.03.016

85. Ojansivu M, Vanhatupa S, Björkvik L, et al. Bioactive glass ions as strong enhancers of osteogenic differentiation in human adipose stem cells. *Acta Biomater*. 2015;21:190-203. doi:10.1016/j.actbio.2015.04.017

86. Madanat R, Moritz N, Vedel E, Svedström E, Aro HT. Radio-opaque bioactive glass markers for radiostereometric analysis. *Acta Biomater*. 2009;5(9):3497-3505. doi:10.1016/j.actbio.2009.05.038

87. Valerio P, Pereira MM, Goes AM, Leite MF. The effect of ionic products from bioactive glass dissolution on osteoblast proliferation and collagen production. *Biomaterials*. 2004;25(15):2941-2948. doi:10.1016/j.biomaterials.2003.09.086

88. Karpov M, Laczka M, Leboy PS, Osyczka AM. Sol–gel bioactive glasses support both osteoblast and osteoclast formation from human bone marrow cells. *J Biomed Mater Res Part A*. 2008;84A(3):718-726. doi:10.1002/jbm.a.31386

89. Icer MA, Gezmen-Karadag M. The multiple functions and mechanisms of osteopontin. *Clin Biochem*. 2018;59:17-24. doi:10.1016/j.clinbiochem.2018.07.003

90. De Diego MA, Coleman NJ, Hench LL. Tensile properties of bioactive fibers for tissue engineering applications. *J Biomed Mater Res*. 2000;53(3):199-203. doi:10.1002/(SICI)1097-4636(2000)53:3<199::AID-JBM2>3.0.CO;2-J

91. Peluso G, Ambrosio L, Cinquegrani M, Nicolais L, Tajana G. Macrophage activation induced by different carbon fiber-epoxy resin composites. *J Biomed Mater Res*. 1991;25(5):637-649. doi:10.1002/jbm.820250507

92. Peluso G, Ambrosio L, Cinquegrani M, Nicolais L, Saiello S, Tajana G. Rat peritoneal immune response to carbon fibre reinforced epoxy composite implants. *Biomaterials*. 1991;12(2):231-235. doi:10.1016/0142-9612(91)90205-O

93. Cheung HY, Lau KT, Lu TP, Hui D. A critical review on polymer-based bio-engineered materials for scaffold development. *Compos Part B Eng*. 2007;38(3):291-300. doi:10.1016/j.compositesb.2006.06.014

94. Gogolewski S, Jovanovic M, Perren SM, Dillon JG, Hughes MK. Tissue response and in vivo degradation of selected polyhydroxyacids: Polylactides (PLA), poly(3-hydroxybutyrate) (PHB), and poly(3-hydroxybutyrate-co-3-hydroxyvalerate) (PHB/VA). *J Biomed Mater Res*. 1993;27(9):1135-1148. doi:10.1002/jbm.820270904

95. Alm JJ, Frantzén JPA, Moritz N, et al. In vivo testing of a biodegradable woven fabric made of bioactive glass fibers and PLGA80-A pilot study in the rabbit. *J Biomed Mater Res - Part B Appl Biomater*. 2010;93(2):573-580. doi:10.1002/jbm.b.31618

96. Zargar Kharazi A, Fathi MH, Manshaei M, Razavi SM. In-vivo evaluation of a partially resorbable poly l-lactic acid/ braided bioactive glass fibers reinforced composite for load bearing fracture fixation. *J Mater Sci Mater Med*. 2020;31(7). doi:10.1007/s10856-020-06394-6

97. Wu P, Wang Y, Sun D, et al. In-vivo histocompatibility and osteogenic potential of biodegradable PLDLA composites containing silica-based bioactive glass fiber. *J Biomater Appl*. 2020;35(1):59-71. doi:10.1177/0885328220911598

98. Medical products - ABMcomposite technology. https://abmcomposite.com/medical/. Accessed October 30, 2020.

99. Wang Y, Wu P, Sun D, et al. Mechanical and degradative properties of PLDLA biodegradable pins with bioactive glass fibers in a beagle model. *Biomed Mater*. 2020;15(3). doi:10.1088/1748-605X/ab772d

100. Lehtonen TJ, Tuominen JU, Hiekkanen E. Resorbable composites with bioresorbable glass fibers for load-bearing applications. in vitro degradation and degradation mechanism. *Acta Biomater*. 2013;9(1):4868-4877. doi:10.1016/j.actbio.2012.08.052

101. Pirhonen E, Grandi G, Törmälä P. Bioactive glass fiber/polylactide composite. *Key Eng Mater*. 2001;192-195:725-728. doi:10.4028/www.scientific.net/kem.192-195.725

102. Ballo AM, Akca E, Ozen T, et al. Effect of implant design and bioactive glass coating on biomechanical properties of fiber-reinforced composite implants. *Eur J Oral Sci*. 2014;122(4):303-309. doi:10.1111/eos.12133

103. Hindié M, Degat MC, Gaudire F, Gallet O, Van Tassel PR, Pauthe E. Pre-osteoblasts on poly(l-lactic acid) and silicon oxide: Influence of fibronectin and albumin adsorption. *Acta Biomater*. 2011;7(1):387-394. doi:10.1016/j.actbio.2010.08.001

104. Zein I, Hutmacher DW, Tan KC, Teoh SH. Fused deposition modeling of novel scaffold architectures for tissue engineering applications. *Biomaterials*. 2002;23(4):1169-1185. doi:10.1016/S0142-9612(01)00232-0

105. Hutmacher DW, Schantz T, Zein I, Ng KW, Teoh SH, Tan KC. Mechanical properties and cell cultural response of polycaprolactone scaffolds designed and fabricated via fused deposition modeling. *J Biomed Mater Res*. 2001;55(2):203-216. doi:10.1002/1097-4636(200105)55:2<203::AID-JBM1007>3.0.CO;2-7

106. Schantz JT, Hutmacher DW, Chim H, Ng KW, Lim TC, Teoh SH. Induction of ectopic bone formation by using human periosteal cells in combination with a novel scaffold technology. *Cell Transplant*. 2002;11(2):125-138. doi:10.3727/096020198389852

107. Olsen-Claire J, Blaker JJ, Roether JA, Boccaccini AR, Schmack G, Gliesche K. Bioglass® coatings on biodegradable poly(3-hydroxybutyrate) (P3HB) meshes for tissue engineering scaffolds. *Materwiss Werksttech*. 2006;37(7):577-583. doi:10.1002/mawe.200500942